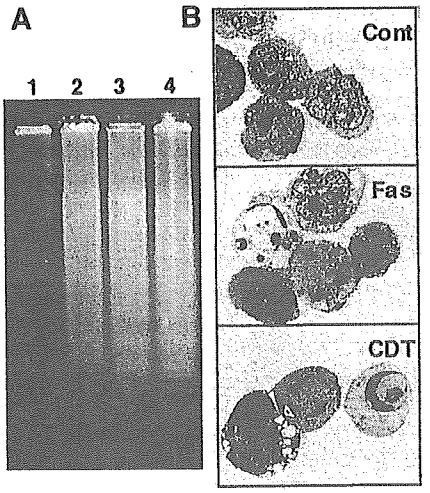

FIG. 3. Apoptotic DNA fragmentation and morphological change in CDT-treated lymphocytes. (A) DNA ladder formation in CDT-treated cells. Jurkat cells were treated with anti-Fas Ab (100 ng/ml) (lane 2), X-ray irradiation (10 Gy) (lane 3), or CDT (100 ng/ml) (lane 4) for 16 h, and chromosomal DNAs were prepared. The extracted DNAs were separated by agarose gel electrophoresis and visualized by staining with ethidium bromide. Lane 1, DNA from untreated Jurkat cells. (B) Ultrastructure of CDT- or anti-Fas Ab-treated lymphocytes. Jurkat cells were treated with CDT (100 ng/ml) for 16 h and subjected to electron microscopic observation as described in Materials and Methods. Cont, control.

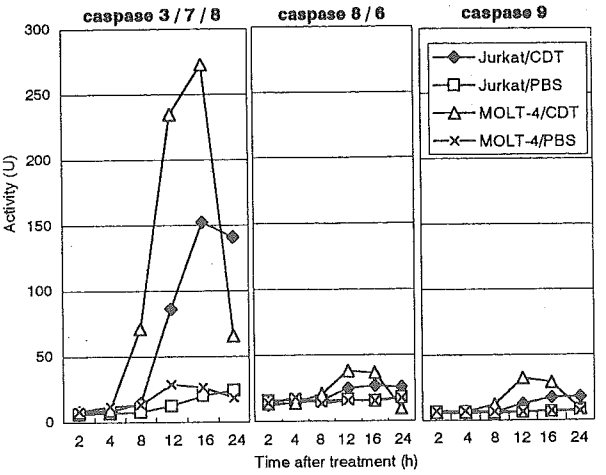

FIG. 4. Caspase activity in CDT-treated lymphocytes. The total protein (10 μg) was extracted from CDT-treated Jurkat or MOLT-4 cells at the indicated times. Caspase activity was measured by incubation of the extract with a fluorogenic substrate for caspase-3, -7, and -8 (left), caspase-8 and -6 (middle), or caspase-9 (right). After incubation, the released 7-amino-4-methylcumarine was measured in spectrophotometer, with excitation at 380 nm and emission at 460 nm. ◆, CDT-treated Jurkat cells; □, PBS-treated Jurkat cells (control); △, CDT-treated MOLT-4; ×, PBS-treated MOLT-4 (control). The experiments were repeated at least three times, and similar results were obtained. Representative results are shown.

such as swelling of the cell body and mitochondria or collapse of the plasma and nuclear membranes, in these cell lines.

Intracellular caspase activities. Apoptosis generally involves the activation of cysteine proteases, or caspases. The activity of sets of the major caspases, caspase-3, -7, and -8, caspase-8 and -6, and caspase-9, in Jurkat and MOLT-4 cells was monitored after CDT treatment. In Jurkat cells, the activity of caspase-3, -7, and -8 started to increase 8 h after treatment of the cells with CDT and significantly increased until 16 to 24 h (Fig. 4). On the other hand, the activity of the caspase-8 and -6 set and caspase-9 slightly increased upon treatment with CDT. Interestingly, caspase activity in MOLT-4 cells started to increase earlier and occurred at a higher level than in Jurkat cells between 4 and 16 h after treatment. After 12 to 16 h, caspase activity in MOLT-4 cells went down in parallel with the appearance of the annexin V^+ PI^- cell population (Fig. 4, Fig. 2B).

Cells retained the phenotype of living cells (annexinV^- PI^-) when the cells were pretreated with a general caspase inhibitor, z-VAD-fmk (100 μM), indicating that z-VAD-fmk is able to nearly completely inhibit CDT-induced apoptosis (Fig. 5A and B). It also turned out that the CDT-induced elevation of caspase activity could be blocked by z-VAD-fmk (Fig. 5C). These results indicated that CDT-induced apoptotic cell death in Jurkat and MOLT-4 cells was mostly dependent on the activation of a caspase(s) until at least 24 h after treatment.

Signaling pathway of caspases. Caspases can be classified into two categories as follows: initiator caspases, including caspase-2, -8, and -9, which are present upstream of the signaling pathway of apoptosis, and effector caspases, which play roles in the cleavage of many regulatory proteins (3). In order to determine the signaling pathway of the caspase(s) in CDT-induced apoptosis, we added a variety of caspase inhibitors and monitored their inhibitory effects on CDT cytotoxicity and apoptotic features in Jurkat cells by using flow cytometry with annexin V-PI double staining. For Fas-mediated apoptosis, caspase-8 was confirmed to be a critical initiator caspase for receptor-mediated apoptosis signaling in Jurkat cells, since the addition of Ac-IETD-CHO, an inhibitor of caspase-8 and -6, significantly inhibited the death of Jurkat cells by an anti-Fas Ab (Fig. 6A and C). On the other hand, inhibitors for caspase-3 (Ac-DMQD-CHO), caspase-8 and -6 (Ac-IETD-CHO), and caspase-9 (Ac-LEHD-CHO) failed to inhibit CDT-induced apoptosis of Jurkat cells (Fig. 6B and C), suggesting that CDT-induced apoptosis might use a different signaling pathway from that of Fas-mediated apoptosis. To determine which caspase(s) among those we tested is actually involved in CDT-induced apoptosis, we analyzed the effects of inhibitors of caspase-1 (Ac-WEHD-CHO), caspase-2 (Ac-VDVAD-CHO), and caspase-3, -7, and -8 (Ac-DEVD-CHO) on CDT-induced apoptosis. The inhibitor of caspase-1 (Ac-WEHD-CHO) had no inhibitory effect on CDT-induced apoptosis of Jurkat cells at concentrations up to 200 μM. On the other hand, CDT-induced apoptosis was dose dependently inhibited by the inhibitor of caspase-2 (VDVAD) or that of caspase-3, -7, and -8 (DEVD) (Fig. 7A and B). However, the combination of inhibitors of caspase-2 (VDVAD) and of caspase-3, -7, and -8 (DEVD) did not show any multiplier effect (Fig. 7C). Together with the fact that inhibitors of caspase-3 (Ac-DMQD-CHO) and caspase-8 and -6 (Ac-IETD-CHO) failed to prevent CDT-induced apoptosis (Fig. 6), our results strongly suggested

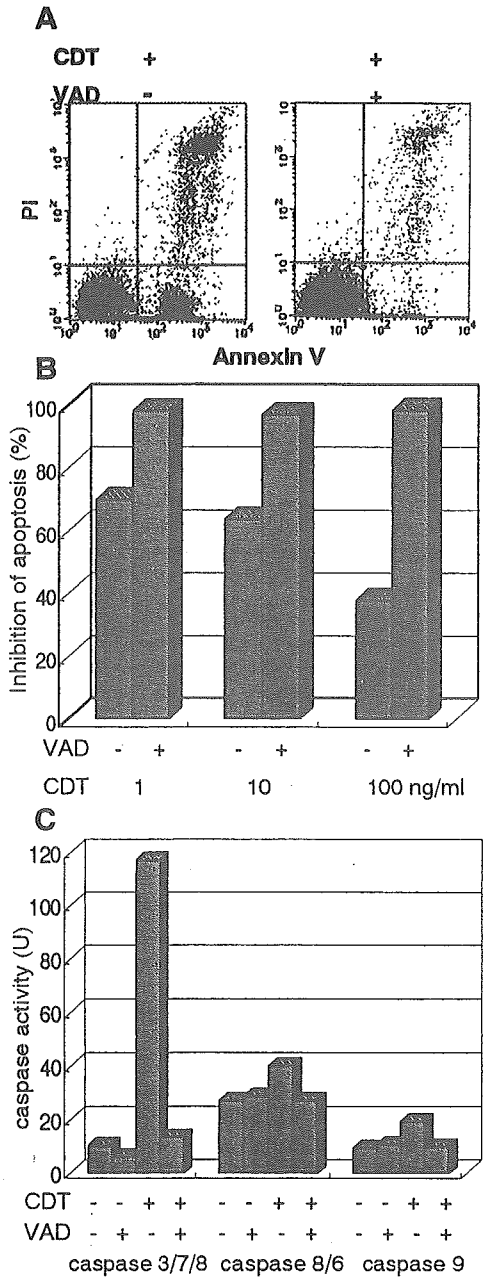

FIG. 5. Effect of general caspase inhibitor on CDT-induced apoptosis. (A) Jurkat cells were preincubated with z-VAD-fmk (100 μM) for 30 min and then were treated with CDT (1, 10, or 100 ng/ml) for 16 h. Cells were stained with FITC-annexin V and PI and analyzed by flow cytometry. The flow cytometry pattern represents CDT (100 ng/ml)-treated lymphocytes with (+) or without (−) z-VAD-fmk. Inhibition of apoptosis was calculated as the relative percentage of living cells, or the population in the LL quadrant (annexin V^- PI^- population). (B) z-VAD-fmk inhibits apoptosis in the cells treated with various concentrations of CDT. (C) Effect of z-VAD-fmk on caspase-3, -7, and -8, caspase-8 and -6, and caspase-9 activity induced by CDTB. Jurkat cells were preincubated with z-VAD-fmk (100 μM) for 30 min and then were treated with CDT (100 ng/ml). Caspase activity was measured as described in Materials and Methods.

that caspase-2 and -7 were mainly involved in the activation of this caspase-dependent apoptotic cascade. We therefore measured the activities of caspase-2 and -7 after CDT treatment for 16 h. To measure caspase-7 activity, we used Ac-DQTD-AMC (substrate for caspase-3 and -7) as a substrate because no caspase-7-specific substrate was available. As shown in Fig. 8A, CDT significantly induced the activation of caspase-2. CDT also induced caspase-3 and -7 activity, but the caspase-3-specific inhibitor Ac-DMQD-CHO did not inhibit the activity at all (Fig. 8A). This clearly indicated that the CDT treatment activated caspase-7. These data suggest that caspase-2 and caspase-7 are really involved in the pathway of CDT-induced apoptotic cell death. It is noteworthy that Ac-VDVAD-CHO (caspase-2 inhibitor) showed an inhibitory effect on caspase-3 and -7 activity. Similarly, Ac-DQTD-CHO (the caspase-3 and -7 inhibitor) clearly inhibited the effect on caspase-2. These results suggest that the caspase-2 and -7 pathways of CDT-induced apoptosis are tightly linked to each other, and they are quite consistent with the results of the experiment on the combination effect of inhibitors of caspase-2 and caspase-3, -7, and -8 (Fig. 7C). The incomplete inhibition of caspase-2 activity by Ac-VDVAD-CHO (caspase-2 inhibitor) implies that another molecule with proteolytic activity similar to that of caspase-2 may be involved in CDT-induced cell death.

To determine whether the mitochondrial pathway is really involved in CDT-induced apoptosis, we analyzed the release of cytochrome *c* from mitochondria in CDT-treated cells. As shown in Fig. 8B, the immunoblotting assay revealed that cytochrome *c* was detectable in the cytosol at 8 h, and more apparently so at 16 h, after CDT treatment of Jurkat cells. The appearance of cytochrome *c* accorded well with the time course of caspase activation, suggesting that the mitochondrial pathway is also involved in CDT-induced apoptosis.

DISCUSSION

In order to investigate CDT-induced apoptosis, we first attempted to establish a cell line model of it. Cytological and biological characterizations of CDT-treated Jurkat and MOLT-4 cells satisfied the apoptosis criteria, such as an increase in membrane conformational changes detected by an increase in the annexin V-positive cell population, intranucleosomal DNA fragmentation, chromatin condensation, and an increase in caspase activity (Fig. 1 to 4). It is noteworthy that the elevation of caspase activity in Jurkat and MOLT-4 cells showed some considerable differences in time course and in activation pattern: the culmination of induced caspase activity was higher in CDT-treated MOLT-4 cells than in similarly treated Jurkat cells. This may suggest that Jurkat and MOLT-4 cells took different apoptotic pathways after exposure to CDT. In this context, it should be noted that Jurkat, but not MOLT-4, cells are deficient in p53 (10). p53 is implicated in the G_2/M block in CDT-treated keratinocytes and fibroblasts (7). The phosphorylation of p53 and other phosphorylation signals could play some role in CDT-induced apoptosis, and the lack of p53 might alter the pathway of apoptosis of Jurkat cells from that of MOLT-4 cells.

We tried to obtain further insights into the understanding of the signaling pathway of CDT-induced apoptosis, especially regarding the caspase cascade(s). Caspases are members of the

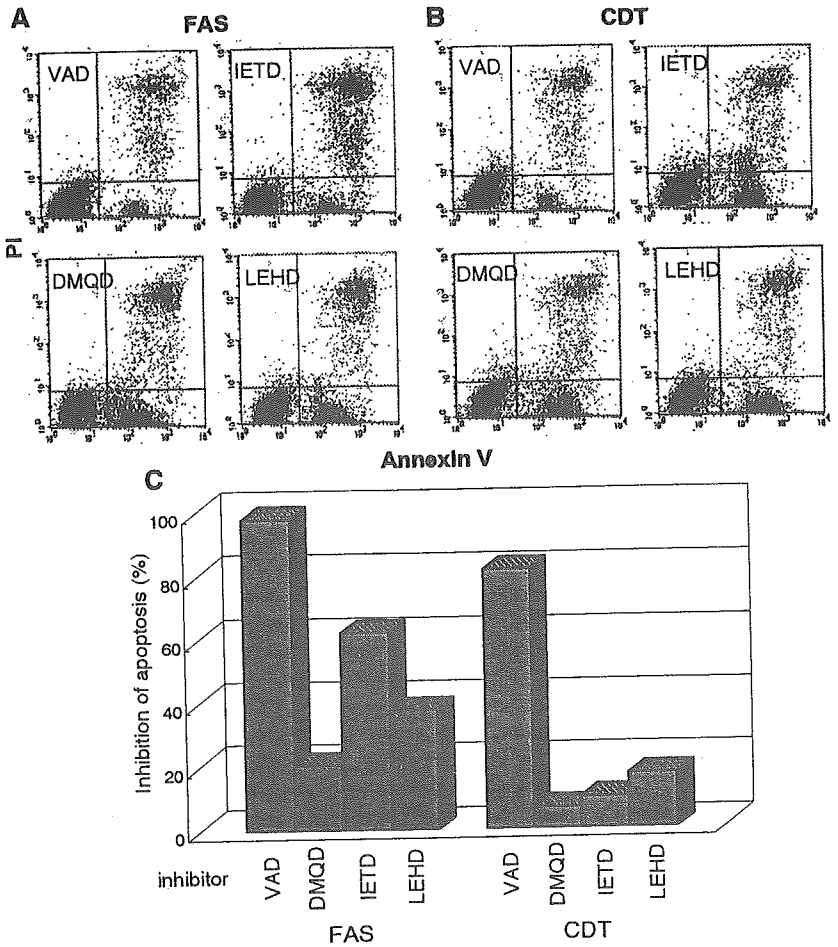

FIG. 6. Effect of various caspase inhibitors on CDT-induced apoptosis. Jurkat cells were preincubated with the indicated inhibitors (100 μM) for 30 min and then were treated with anti-Fas Ab (100 ng/ml) (A) or CDT (100 ng/ml) (B). After 16 h, cells were stained with FITC-annexin V and PI and analyzed by FACScan. The inhibitors used were VAD (general caspase inhibitor), DMQD (caspase-3 inhibitor), IETD (caspase-8 and -6 inhibitor), and LEHD (caspase-9 inhibitor). (A and B) Representative flow cytometry patterns. (C) Effect of caspase inhibitors on apoptosis induced by anti-Fas Ab (left) or CDT (right). Inhibition of apoptosis was defined as the relative percentage of normal living cells (annexin V^- PI^-).

aspartate-specific cysteine protease family which play a critical role in apoptosis (6, 39). They are composed of two major subfamilies, initiator caspases and effector caspases, based on the presence or absence of a large prodomain in the amino-terminal region (33). Initiator caspases generally act upstream of the proteolytic cascade, while effector caspases act downstream and are involved in the cleavage of specific cellular substrate proteins (41). Once processed, the substrates induce morphological changes characteristic of the apoptotic process (8, 11). The long prodomains of the initiator caspases trigger and/or facilitate the activation of proenzymes through interactions with adaptor molecules (13). Caspase-2, -8, -9, and -10 generally act as initiator caspases upstream of the cascade of effector caspases with small prodomains, such as caspase-3, -6, and -7 (26). Among the caspases, caspase-8, -9, and -10 play a fundamental role in transducing the specific apoptotic signal, and they cleave and activate effector procaspase-3, -6, and -7 (4). Effector caspases, in turn, cleave various proteins, leading to morphological and biochemical features characteristic of apoptosis. Recently, it has become clear that caspase-9 is involved in the apoptotic pathway that relys on mitochondrial dysfunction (15). Caspase-8 and -10 are involved in the apoptosis pathway mediated by death receptors (2).

Our results indicated that inhibitors of caspase-2 and -7 showed inhibitory effects on CDT-induced apoptosis. Several bacterial toxins are known to induce apoptosis through caspase-dependent pathways, although the exact molecular mechanism of the signaling cascade has not been well characterized. For instance, Shiga toxin and Shiga-like toxin have been demonstrated to activate caspase-2, -3, -6, -8, and -9 (5, 17, 18). It was suggested that these toxins use the caspase cascade involved in Fas-mediated apoptosis. Other toxins, such as *E. coli* heat-labile enterotoxin (32), *Clostridium difficile* toxin B (29), diphtheria toxin (19), and *Mannheimia haemolytica* leukotoxin (23), were shown to induce caspase-3. However, a detailed caspase cascade induced by bacterial toxins has not been well established. To our knowledge, this is the first report that a bacterial toxin preferentially utilizes caspase-2 and -7 in

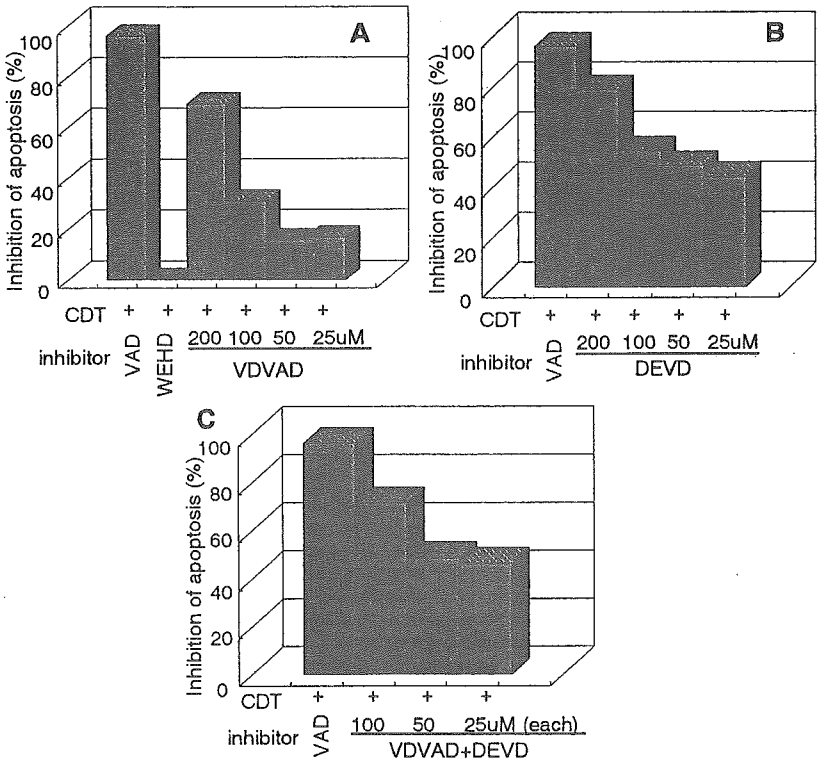

FIG. 7. Dose-dependent inhibitory effects of caspase inhibitors on CDT-induced apoptosis. Jurkat cells were preincubated with various concentrations of caspase inhibitors (25, 50, 100, and 200 μM) for 30 min and then were treated with CDT (100 ng/ml). The inhibitors used were WEHD (caspase-1 inhibitor), VDVAD (caspase-2 inhibitor), and DEVD (caspase-3, -7, and -8 inhibitor). After 16 h, cells were stained with FITC-annexin V and PI and analyzed by flow cytometry. Panels show the relative inhibition of CDT-induced apoptosis with VDVAD (A), DEVD (B), and VDVAD and DEVD (C). Inhibition of apoptosis was defined as the relative percentage of living cells (annexin V^- PI^-). VAD (general caspase inhibitor) and WEHD were used at concentrations of 100 and 200 μM, respectively.

the signaling pathway for apoptosis. In recent studies, caspase-2 was implicated in the release of cytochrome *c* from mitochondria in stress-induced apoptotic pathways (16, 22, 27, 30). One such stress-inducing agent is a topoisomerase II poison, etoposide, that induces double-stranded DNA breaks in cells. Robertson et al. (30) demonstrated that etoposide-induced DNA damage induces activation of caspase-2 and hence results in cytochrome *c* release from mitochondria and subsequent apoptosis. It is interesting that a possible mechanism by which CDT can induce cytopathic effects involves DNA strand breaks induced by its putative DNase activity (12, 20). Such CDT-induced DNA damage may trigger the mitochondrial cascade including caspase-2 and -7. A recent report has indicated the requirement of caspase-2 for the initiation of stress-induced apoptosis prior to mitochondrial permeabilization (22). In our case, CDT-induced DNA damage may directly activate caspase-2 and then induce the mitochondrial cascade, probably followed by caspase-7 activation. Caspase-7 is a late signal transducer and one of the members of the apoptosome complex which is activated by mitochondrial stress (3). Both caspase-2 and -7 are involved in stress-induced cascades, suggesting that CDT-induced apoptosis is related to the mitochondrial pathway. Our present results indicate that CDT can induce mitochondrial membrane permeabilization, resulting in the release of cytochrome *c*, and that this mitochondrial pathway is highly involved in CDT-induced apoptosis. This is quite in agreement with an experiment showing that Bcl-2 overexpression reduces apoptosis in a CDT-treated human B lymphoblastoid cell line, JY (35).

Fas ligation on the cell surface induces apoptosis through the receptor-mediated signaling pathway, which involves caspase-8 as an initiation signal (2). The fact that caspase-8 inhibitor blocked Fas-mediated apoptosis in Jurkat cells (Fig. 6) indicated that the Fas-dependent apoptotic pathway was active in this cell line. In contrast, no inhibitory effect of caspase-8 inhibitor on CDT-induced apoptosis was observed in Jurkat cells, suggesting that the cytotoxic effect of CDT does not require the activation of death receptors on the cell surface.

Since CDT is able to induce apoptosis of activated T cells, this toxin may play an important role in that the bacteria evade T-cell immune responses in the periodontal pocket. It is conceivable that CDT produced by this pathogen exacerbates local inflammation by inducing apoptotic cell death of T lymphocytes that are responsible for the clearance of bacteria from the periodontal pocket. Further studies on the effect of CDT on the caspase network should unveil the CDT-related signal transduction pathway in T-lymphocyte apoptosis that may lead to the suppression of immune responses to the pathogen.

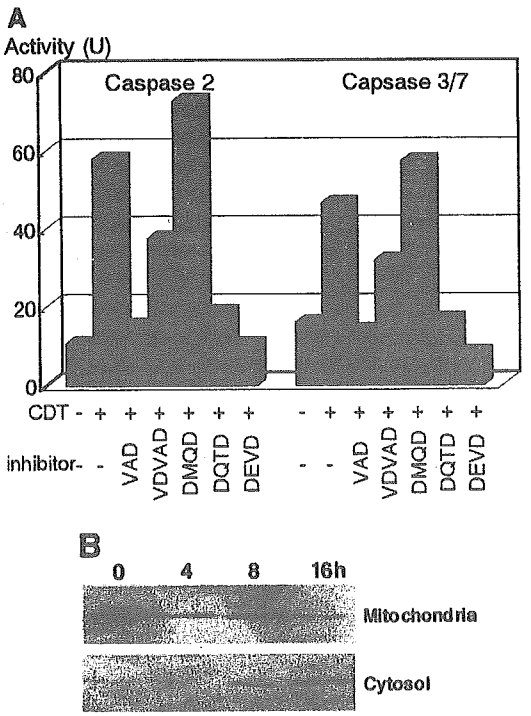

FIG. 8. Elevation of caspase-2 or -7 activity and cytochrome *c* release by CDT treatment. (A) Jurkat cells were preincubated with the indicated inhibitor (100 μM) for 30 min and then were treated with CDT (100 ng/ml) for 16 h. The inhibitors used were VAD (general caspase inhibitor), VDVAD (caspase-2 inhibitor), DMQD (caspase-3 inhibitor), DQTD (caspase-3 and -7 inhibitor), and DEVD (caspase-3, -7, and -8 inhibitor). Caspase activity was measured as described in Materials and Methods. (B) Cytosol and mitochondrial fractions were extracted from Jurkat cells that were treated with CDT (100 ng/ml) for 0, 4, 8, and 16 h and were subsequently immunoblotted with an anti-cytochrome *c* Ab followed by a horseradish peroxidase-conjugated secondary Ab. The bands of cytochrome *c* were visualized by ECL.

ACKNOWLEDGMENTS

We thank Kei Nakachi, Donald G. MacPhee, and Seishi Kyoizumi at the Department of Radiobiology and Molecular Epidemiology, Radiation Effects Research Foundation, for helpful suggestions. We thank the Research Facilities, Hiroshima University School of Dentistry and School of Medicine, for the use of facilities.

This study was supported in part by a Grant for Development of Highly Advanced Medical Technology (A) and by a Grant-in-Aid for Scientific Research (B) from the Ministry of Education, Science, Sports and Culture of Japan.

REFERENCES

1. **Alby, F., R. Mazars, J. De Rycke, E. Guillou, V. Baldin, J.-M. Darbon, and B. Ducommun.** 2001. Study of the cytolethal distending toxin (CDT)-activated cell cycle checkpoint. Involvement of the CHK2 kinase. FEBS Lett. **491**:261–265.
2. **Ashkenazi, A., and V. M. Dixit.** 1998. Death receptors: signaling and modulation. Science **281**:1305–1308.
3. **Bratton, S. B., M. Macfarlane, K. Cain, and G. M. Cohen.** 2000. Protein complexes activate distinct caspase cascades in death receptor and stress induced apoptosis. Exp. Cell Res. **256**:27–33.
4. **Budihardjo, I., H. Oliver, M. Lutter, X. Luo, and X. Wang.** 1999. Biochemical pathways of caspase activation during apoptosis. Annu. Rev. Cell Dev. Biol. **15**:269–290.
5. **Ching, J. C., N. L. Jones, P. J. Ceponis, M. A. Karmali, and P. M. Sherman.** 2002. *Escherichia coli* Shiga-like toxins induce apoptosis and cleavage of poly(ADP-ribose) polymerase via in vitro activation of caspases. Infect. Immun. **70**:4669–4677.
6. **Cohen, G. M.** 1997. Caspases: the executioners of apoptosis. Biochem. J. **326**:1–16.
7. **Cortes-Bratti, X., C. Karlsson, T. Lagergard, M. Thelestam, and T. Frisan.** 2001. The *Haemophilus ducreyi* cytolethal distending toxin induces cell cycle arrest and apoptosis via the DNA damage checkpoint pathways. J. Biol. Chem. **276**:5296–5302.
8. **Cryns, V., and J. Yuan.** 1998. Proteases to die for. Genes Dev. **12**:1551–1570.
9. **Deng, K., J. L. Latimer, D. A. Lewis, and E. J. Hansen.** 2001. Investigation of the interaction among the components of the cytolethal distending toxin of *Haemophilus ducreyi*. Biochem. Biophys. Res. Commun. **20**:609–615.
10. **Dreyfus, D. H., M. Nagasawa, C. A. Kelleher, and E. W. Gelfand.** 2000. Stable expression of Epstein-Barr virus BZLF-1-encoded ZEBRA protein activates p53-dependent transcription in human Jurkat T-lymphoblastoid cells. Blood **96**:625–634.
11. **Earnshaw, W. C., L. M. Martins, and S. H. Kaufmann.** 1999. Mammalian caspases: structure, activation, substrates, and functions during apoptosis. Annu. Rev. Biochem. **68**:383–424.
12. **Elwell, C. A., K. Chao, K. Patel, and L. A. Dreyfus.** 2001. *Escherichia coli* CdtB mediates cytolethal distending toxin cell cycle arrest. Infect. Immun. **69**:3418–3422.
13. **Fesik, S. W.** 2000. Insights into programmed cell death through structural biology. Cell **103**:273–282.
14. **Frisk, A., M. Labens, C. Johansson, H. Ahmed, L. Svensson, K. Ahlman, and T. Lagergard.** 2001. The role of different protein components from the *Haemophilus ducreyi* cytolethal distending toxin in the generation of cell toxicity. Microb. Pathog. **30**:313–324.
15. **Green, D. R.** 2000. Apoptotic pathways: paper wraps stone blunts scissors. Cell **102**:1–4.
16. **Guo, Y., S. M. Srinivasula, A. Druilhe, T. Fernandes-Alnemri, and E. S. Alnemri.** 2002. Caspase-2 induces apoptosis by releasing proapoptotic proteins from mitochondria. J. Biol. Chem. **277**:13430–13437.
17. **Kiyokawa, N., T. Mori, T. Taguchi, M. Saito, K. Mimori, T. Suzuki, T. Sekino, N. Sato, H. Nakajima, Y. U. Katagiri, T. Takeda, and J. Fujimoto.** 2001. Activation of the caspase cascade during Stx-1-induced apoptosis in Burkitt's lymphoma cells. J. Cell. Biochem. **81**:128–142.
18. **Kojio, S., H. Zhang, M. Ohmura, F. Gondaira, N. Kobayashi, and T. Yamamoto.** 2000. Caspase-3 activation and apoptosis induction coupled with the retrograde transport of Shiga toxin: inhibition by brefeldin A. FEMS Immunol. Med. Microbiol. **29**:275–281.
19. **Komatsu, N., T. Oda, and T. Muramatsu.** 1998. Involvement of both caspase-like proteases and serine proteases in apoptotic cell death induced by ricin, modeccin, diphtheria toxin, and pseudomonas toxin. J. Biochem. (Tokyo) **124**:1038–1044.
20. **Lara-Tejero, M., and J. E. Galan.** 2000. A bacterial toxin that controls cell cycle progression as a deoxyribonuclease I-like protein. Science **290**:354–357.
21. **Lara-Tejero, M., and J. E. Galan.** 2001. CdtA, CdtB, and CdtC form a tripartate complex that is required for cytolethal distending toxin activity. Infect. Immun. **69**:4358–4365.
22. **Lassus, P., X. Opitz-Araya, and Y. Lazebnik.** 2002. Requirement for caspase-2 in stress-induced apoptosis before mitochondrial permeabilization. Science **297**:1352–1354.
23. **Leite, F., S. O'Brien, M. J. Sylte, T. Page, D. Atapattu, and C. J. Czuprynski.** 2002. Inflammatory cytokines enhance the interaction of *Mannheimia haemolytica* leukotoxin with bovine peripheral blood neutrophils in vitro. Infect. Immun. **70**:4336–4343.
24. **Lewis, D. A., M. K. Stevens, J. L. Latimer, C. K. Ward, K. Deng, R. Blick, S. R. Lumbley, C. A. Ison, and E. J. Hansen.** 2001. Characterization of *Haemophilus ducreyi cdtA*, *cdtB*, and *cdtC* mutants in in vitro and in vivo systems. Infect. Immun. **69**:5626–5634.
25. **Mangan, D. F., N. S. Taichman, E. T. Lally, and S. M. Wahl.** 1991. Lethal effects of *Actinobacillus actinomycetemcomitans* leukotoxin on human T lymphocytes. Infect. Immun. **59**:3267–3272.
26. **Nicholson, D. W., and N. A. Thornberry.** 1997. Caspases: killer proteases. Trends Biochem. Sci. **22**:299–306.
27. **Paroni, G., C. Henderson, C. Schneider, and C. Brancolini.** 2002. Caspase-2 can trigger cytochrome *c* release and apoptosis from the nucleus. J. Biol. Chem. **277**:15147–15161.
28. **Pickett, C. L., and C. A. Whitehouse.** 1999. The cytolethal distending toxin family. Trends Microbiol. **7**:292–297.
29. **Qa'Dan, M., M. Ramsey, J. Daniel, L. M. Spyres, B. Safiejko-Mroczka, W. Ortiz-Leduc, and J. D. Ballard.** 2002. *Clostridium difficile* toxin B activates dual caspase-dependent and caspase-independent apoptosis in intoxicated cells. Cell. Microbiol. **4**:425–434.
30. **Robertson, J. D., M. Enoksson, M. Suomela, B. Zhivotovsky, and S. Orrenius.** 2002. Caspase-2 acts upstream of mitochondria to promote cytochrome *c* release during etoposide-induced apoptosis. J. Biol. Chem. **277**:29803–29809.
31. **Saiki, K., K. Konishi, T. Gomi, T. Nishihara, and M. Yoshikawa.** 2001. Reconstitution and purification of cytolethal distending toxin of *Actinobacillus actinomycetemcomitans*. Microbiol. Immunol. **45**:497–506.
32. **Salmond, R. J., R. S. Pitman, E. Jimi, M. Soriani, T. R. Hirst, S. Ghosh, M. Rincon, and N. A. Williams.** 2002. $CD8^+$ T cell apoptosis induced by *Esch-*

erichia coli heat-labile enterotoxin B subunit occurs via a novel pathway involving NF-kappaB-dependent caspase activation. Eur. J. Immunol. **32:** 1737–1747.

33. **Salvesen, G. S., and V. M. Dixit.** 1999. Caspase activation: the induced-proximity model. Proc. Natl. Acad. Sci. USA **96:**10964–10967.
34. **Shenker, B. J., R. H. Hoffmaster, T. L. Mckay, and D. R. Demuth.** 2000. Expression of the cytolethal distending toxin (Cdt) operon in *Actinobacillus actinomycetemcomitans*: evidence that the CdtB protein is responsible for G_2 arrest of the cell cycle in human T cells. J. Immunol. **165:**2612–2618.
35. **Shenker, B. J., R. H. Hoffmaster, A. Zekavat, N. Yamaguchi, E. T. Lally, and D. Demuth.** 2001. Induction of apoptosis in human T cells by *Actinobacillus actinomycetemcomitans* cytolethal distending toxin is a consequence of G_2 arrest of the cell cycle. J. Immunol. **167:**435–441.
36. **Shenker, B. J., T. McKay, S. Datar, M. Miller, R. Chowhan, and D. Demuth.** 1999. *Actinobacillus actinomycetemcomitans* immunosuppressive protein is a member of the family of cytolethal distending toxins capable of causing a G_2 arrest in human T cells. J. Immunol. **162:**4773–4780.
37. **Shenker, B. J., L. Vitale, and C. King.** 1995. Induction of human T cells that coexpress CD4 and CD8 by an immunomodulatory protein produced by *Actinobacillus actinomycetemcomitans.* Cell. Immunol. **164:**36–46.
38. **Slots, J., H. S. Reynolds, and R. J. Genco.** 1980. *Actinobacillus actinomycetemcomitans* in human periodontal disease: a cross-sectional microbiological investigation. Infect. Immun. **29:**1013–1020.
39. **Stennicke, H. R., and G. S. Salvesen.** 1997. Biochemical characteristics of caspases-3, -6, -7, and -8. J. Biol. Chem. **272:**25719–25723.
40. **Sugai, M., T. Kawamoto, S. Y. Peres, Y. Ueno, H. Komatsuzawa, T. Fujiwara, H. Kurihara, H. Suginaka, and E. Oswald.** 1998. The cell cycle-specific growth-inhibitory factor produced by *Actinobacillus actinomycetemcomitans* is a cytolethal distending toxin. Infect. Immun. **66:**5008–5019.
41. **Thornberry, N. A., and Y. Lazebnik.** 1998. Caspases: enemies within. Science **281:**1312–1316.

Editor: V. J. DiRita

Expression Characteristics and Stimulatory Functions of CD43 in Human CD4$^+$ Memory T Cells: Analysis Using a Monoclonal Antibody to CD43 That Has a Novel Lineage Specificity[1]

Seishi Kyoizumi,[2]* Takaaki Ohara,† Yoichiro Kusunoki,* Tomonori Hayashi,* Kazuaki Koyama,* and Naohiro Tsuyama‡

We have used HSCA-2, an mAb that recognizes a sialic acid-dependent epitope on the low molecular mass (~115-kDa) glycoform of CD43 that is expressed in resting T and NK cells, to examine the expression characteristics and stimulatory functions of CD43 in human CD4$^+$ memory T cells. Having previously reported that the memory cells that respond to recall Ags in a CD4$^+$CD45RO$^+$ T cell population almost all belong to a subset whose surface CD43 expression levels are elevated, we now find that exposing these same memory T cells to HSCA-2 mAb markedly increases their proliferative responsiveness to recall Ags. We think it unlikely that this increase in responsiveness is a result of CD43-mediated monocyte activation, especially given that the HSCA-2 mAb differs from all previously used CD43 mAbs in having no obvious binding specificity for monocyte CD43. Predictably, treatment with HSCA-2 mAb did not lead to significant recall responses in CD4$^+$CD45RO$^+$ T cells, whose CD43 expression levels were similar to or lower than those of naive cells. Other experiments indicated that the HSCA-2 mAb was capable of enhancing the proliferative responsiveness of CD4$^+$ memory T cells that had been exposed to polyclonal stimulation by monocyte-bound CD3 mAb and could also act in synergy with CD28 mAb to enhance the responsiveness of CD4$^+$ T cells to CD3 stimulation. Taken together, these findings suggest that the CD43 molecules expressed on CD4$^+$ memory T cells may be capable of enhancing the costimulatory signaling and hence providing accessory functions to TCR-mediated activation processes. *The Journal of Immunology,* **2004, 172: 7246–7253.**

CD43 (leukosialin) is a highly glycosylated transmembrane protein that is expressed in all hemopoietic cells except resting mature B cells and erythrocytes (1, 2). All CD43 molecules possess extracellular domains that consist of multiple *O*-linked carbohydrate chains (3) and show considerable m.w. heterogeneity due to differential glycosylation (4). Even within T cell populations there are at least two glycoforms of CD43 that are recognized by different mAbs. The lighter of these glycoforms has a molecular mass of 95–115 kDa, whereas that of that heavier one is between 130 and 135 kDa (5, 6). Interestingly, the heavier glycoform contains core 2 *O*-glycans, appears to be up-regulated during T cell activation (5, 7), and can be used to distinguish between memory and effector CD8$^+$ T cells in mice (8, 9). It is not yet clear exactly what CD43 does in T cells, however, especially in view of the continued existence of a number of unresolved controversies about its roles in such key processes as cell adhesion, cell death, and costimulation in TCR signaling (10).

It has, for instance, been claimed that CD43 molecules may have antiadhesive as well as proadhesive functions in T cell trafficking (9, 11–14). It has also been claimed that up-regulation of CD43 expression can have a negative effect on activation-induced cell death of T cells (15), and that Ab-mediated cross-linking of CD43 induces apoptosis of Jurkat T cells (16). CD43 also appears to play a role in T cell activation, but precisely what role remains unclear. There are, for example, Ab cross-linking experiments involving CD43 that suggest that it may have a costimulatory role in vitro (17) and act in association with the phosphorylation of signal-transducing molecules in T cell activation (18–20); other experiments using CD43-deficient mice suggest, on the contrary, that CD43 has either a negative regulatory role as a steric barrier (21) or possibly even no significant role at all (22) in T cell activation. There are several recent reports suggesting that molecular complexes between CD43 and cytoskeletal adaptor proteins are probably excluded from the immunological synapse in T cell activation in vitro (23–25) and in vivo (26). Some of these reports include suggestions that this relocalization of CD43 is necessary for activation-induced cytokine production (23, 27), although there is at least one recent study that comes to precisely the opposite conclusion (28). The functional significance of redistribution of CD43 in T cell activation is therefore very unclear. Nevertheless, given that CD43 expression levels appear to be considerably elevated in memory T cell populations in humans (29–31) and mice (15), it seems reasonable to assume that CD43 has an important part to play in one or more aspects of the memory T cell responses.

*Laboratory of Immunology, Department of Radiobiology/Molecular Epidemiology, Radiation Effects Research Foundation, Hiroshima, Japan; †Life Science Laboratories, Life Science RD Center, Kaneka Corp., Takasago, Japan; and ‡Cellular Signal Analysis, Department of Bio-Signal Analysis, Applied Medical Engineering Science, Yamaguchi University Graduate School of Medicine, Ube City, Japan

Received for publication November 11, 2003. Accepted for publication April 2, 2004.

The costs of publication of this article were defrayed in part by the payment of page charges. This article must therefore be hereby marked *advertisement* in accordance with 18 U.S.C. Section 1734 solely to indicate this fact.

[1] This publication is based on research performed at the Radiation Effects Research Foundation (RERF), Hiroshima and Nagasaki, Japan. RERF is a private nonprofit foundation funded equally by the Japanese Ministry of Health, Labor, and Welfare (MHLW) and the U.S. Department of Energy, the latter through the National Academy of Sciences. This work was supported by RERF Research Protocols 1-93 and 4-02 and in part by funds for Research Promotion on AIDS Control from MHLW.

[2] Address correspondence and reprint requests to Dr. Seishi Kyoizumi, Laboratory of Immunology, Department of Radiobiology/Molecular Epidemiology, Radiation Effects Research Foundation, 5-2 Hijiyama Park, Minami Ward, Hiroshima 732-0815, Japan. E-mail address: kyoizumi@rerf.or.jp

0022-1767/04/$02.00

We have recently described how HSCA-2, a novel CD43 mAb, can be used for the classification of human $CD4^+CD45RO^+$ memory T cells into three subsets on the basis of differences in their CD43 expression (31). In this classification, cells of the first of the three subsets (the M1 subset) express elevated levels of CD43, whereas cells of the M2 subset express CD43 levels similar to those of naive cells, and cells of the M3 subset express reduced CD43 levels. We also found that the M1 subset contains the highest proportion of recall Ag-reactive precursors and secretes substantially more IFN-γ and IL-4. The majority of effector memory T cells ($CCR7^-$) (32) are assumed to belong to this subset (31). However, as ~70% of the cells in the M1 subset express CCR7, the subset may also contain central memory T cells. The M2 subset cells are less mature memory cells that retain longer telomeres than do cells of the M1 and M3 subsets, and their memory functionality (including recall Ag reactivity) appears to be marginal (31). The M3 subset consists of cells that are anergic to TCR-mediated stimuli and prone to apoptosis (31). As the level of CD43 expression is correlated with recall Ag reactivity, it is possible that CD43 molecules will prove to have some accessory role in the activation of human $CD4^+$ memory T cells.

In this paper we describe immunological properties and expression characteristics of the CD43 molecules that are recognized by HSCA-2 mAb. We go on to examine the functional properties of these molecules in the proliferative responses of $CD4^+$ memory T cells. The results described in this report demonstrate that the HSCA-2 mAb specifically recognizes a neuraminidase-sensitive epitope of a low molecular mass glycoform (115 kDa) of CD43 that is predominantly expressed in lymphoid populations. It is also suggested that the CD43 glycoform recognized by HSCA-2 mAbs could play an accessory part in the recall Ag-specific responses of mature $CD4^+$ memory T cells (i.e., M1 subset cells). HSCA-2 mAb has therefore proven to be a useful molecular probe for both the classification and the functional analysis of human $CD4^+$ memory T cells. The implications of our work for the involvement of CD43-mediated stimulatory signaling in the activation of $CD4^+$ T cells are discussed.

Materials and Methods

Production of HSCA-2 mAb

The HSCA-2 hybridoma is a product of the fusion of NS1 mouse myeloma cells with splenocytes from BALB/c mice immunized by injection of human KG-1 cells (31). Immunization, fusion, selection, and cloning protocols were essentially as described previously (33). Hybridoma supernatants were initially screened for reactivity with KG-1 cells by indirect immunofluorescence. The HSCA-2 hybridoma was selected for further study because of its unique specificity of reactivity with PBMC and cord blood $CD34^+$ stem cells. Isotype characterization showed that the HSCA-2 mAb was of the IgG1 subclass. Ascites fluid was obtained from SCID mice injected with the HSCA-2 hybridoma. After purification from ascites fluid by DE52 ion exchange chromatography, HSCA-2 mAb was labeled with FITC (Sigma-Aldrich, St. Louis, MO) for flow cytometry. Fab of HSCA-2 mAb were prepared by digestion with papain (34). This mAb was filed for participation in the Eighth International Workshop and Conference on Human Leukocyte Differentiation Ags (to be held in Adelaide, Australia).

Other mAbs

Unconjugated CD28 mAb (clone CD28.2) (35), used for T cell culture, was purchased from Coulter-Immunotech (Marseilles, France). Unconjugated and FITC-conjugated CD43 mAbs, DFT-1 (1), L10 (36), and 1G10 (37), were obtained from Coulter-Immunotech, Caltag Laboratories (Burlingame, CA), and BD PharMingen (San Diego, CA), respectively. PE-labeled CD4, CD8, CD14, CD19, and CD56 mAbs and PerCP-labeled CD4 and CD8 mAbs were purchased from BD Biosciences (San Jose, CA). PE-labeled CD45RO mAb was obtained from Caltag Laboratories.

Transfection of CD43 cDNA

Total RNA of KG-1 cells was isolated with TRIzol reagent (Invitrogen, Carlsbad, CA). First-strand cDNA primed with oligo$(dT)_{30}$ was synthesized using SuperScript II reverse transcriptase (Invitrogen). CD43 cDNA was PCR-amplified with the primers 5′-ctcttgctcctgcctgtttgc-3′ and 5′-catggtggtgggtgcctgtaa-3′ using Advantage cDNA polymerase mix (Clontech Laboratories, Palo Alto, CA) and cloned into pCR2.1 TA cloning vector (Invitrogen). The sequence-verified clone was recloned into the *Eco*RI site of pIRESneo (Clontech Laboratories) and designated pIRESneo hCD43. Subsequently, 30 μg of pIRESneo hCD43 or pIRESneo (negative control) was electroporated into 2×10^6 HeLa cells in 200 μl of PBS by GenePulser (Bio-Rad, Hercules, CA) at 0.7 kV and 25 μF. Cells were treated with 1 mg/ml G418 for 2 wk. Drug-resistant colonies were selected and expanded to confirm CD43 expression by flow cytometry. HeLa transfectant cells expressing high levels of CD43 were isolated by a cell sorter for additional experiments.

Cell preparations and flow cytometry

For direct immunofluorescence of cultured cell lines, 2×10^5 CD43- or mock-transfected HeLa and KG-1 cells were stained with 1 μg of FITC-labeled HSCA-2, DFT-1, and MOPC21 mAbs for 45 min on ice. For the analyses of CD43 glycoepitopes, 2×10^6 KG-1 cells were treated with neuraminidase (0.1 U/ml in PBS) for 30 min at 37°C. For competitive inhibition, KG-1 cells were pretreated with various amounts of HSCA-2 or DFT-1 mAbs (12.5–200 μg/ml) for 1 h on ice and then stained with FITC-labeled HSCA-2 and DFT-1 mAbs for 45 min. FACScan (BD Biosciences) was used for flow cytometric analyses.

For flow cytometry of human blood cells, PBMCs from healthy adult volunteers ($n = 6$) and cord blood mononuclear cells ($n = 3$) were isolated by density centrifugation in Ficoll-Hypaque (density, 1.077 g/ml; ICN Biomedical, Aurora, OH). Granulocytes were isolated by double-layered density centrifugation in Ficoll-Hypaque (density, 1.077 and 1.119 g/ml; Wako Pure Chemical, Osaka, Japan) according to the manufacturer's instructions. For isolation of monocytes, $CD14^+$ cells were purified from PBMCs by positive enrichment using autoMACS (Miltenyi Biotec, Bergish Gladbach, Germany) according to the manufacturer's instructions. Enriched monocytes also were used for immunoprecipitation and proliferation assay, as described below.

For single-color analysis of purified monocytes and granulocytes, cells were stained with FITC-labeled CD43 mAbs and analyzed by flow cytometry with a gate in a region for monocytes or granulocyte fractions on the forward and side light scatter profiles. For two-color analysis of lymphocytes, PBMCs were stained with PE-labeled CD4, CD8, CD19, and CD56 in combination with FITC-labeled CD43 mAbs. Cord blood mononuclear cells were stained with FITC-labeled CD43 and PE-labeled CD34 mAbs. For triple-color analysis, PBMCs were stained with FITC-labeled CD43, PE-conjugated CD45RO, and PerCP-labeled CD4 mAbs. $CD4^+$ lymphocytes were gated on forward/side scatter and PerCP fluorescence. The proportions of $CD4^+$ $CD45RO^-$ cells (RO^- subset) and $CD4^+$ $CD45RO^+$ cells expressing high (M1 subset), intermediate (M2), and low (M3) levels of CD43 were measured by flow cytometry with FACScan (see Fig. 4).

For preparation of activated $CD4^+$ T cells, MACS-purified $CD4^+$ T cells were stimulated with immobilized anti-CD3 mAb (OKT-3) in the presence of IL-2 (10 ng/ml) for 4 days in RPMI 1640 supplemented with 10% FCS. Immobilized CD3 mAb was prepared by binding OKT3 mAb (10 μg/ml in sodium bicarbonate buffer, pH 9.6) in 24-well plates at room temperature for 2 h, then washing the plates with RPMI 1640 supplemented with 10% FCS.

For isolation of the four $CD4^+$ T cell subsets, M1, M2, M3, and $CD45RO^-$, $CD4^+$ cells were purified by negative enrichment using MACS as described previously (31). MACS-purified $CD4^+$ T cells were stained with FITC-labeled HSCA-2 and PE-labeled CD45RO mAbs. After incubation with propidium iodine at 10 μg/ml for 15 min to gate out dead cells, $CD4^+$ T cells in the four subsets were sorted by a single laser cell sorter (FACStar; BD Biosciences). During cell sorting, stained and sorted cell suspensions were maintained at 4°C by a cooling circulation system.

Cell proliferation assay

For proliferative response to recall Ags, PBMCs (5×10^4 cells/well) in 96-well, flat-bottom plastic plates were stimulated with tuberculosis purified protein derivative (PPD;[3] Connaught Laboratories, Ontario, Canada) or tetanus toxoid (TT; Calbiochem, La Jolla, CA) at 5 μg/ml. For total and subset $CD4^+$ T cells, T cells (5×10^4 cells/well) were stimulated with

[3] Abbreviations used in this paper: PPD, purified protein derivative; TT, tetanus toxoid.

these recall Ags in the presence of autologous monocytes (2.5×10^4 cells/well) that were previously isolated using autoMACS with anti-CD14 Ab (Miltenyi Biotec) and irradiated with x-ray at 30 Gy. The culture medium used for this assay was RPMI 1640 supplemented with 10% human serum. For proliferative responses to anti-CD3 mAb, total $CD4^+$ T cells or sorted subset T cells were stimulated with various concentrations of soluble CD3 (OKT-3) mAb (0.0001–1 μg/ml) in the presence of autologous monocytes. The culture medium used for this assay was RPMI 1640 medium supplemented with 10% FCS.

The effects of CD43 (0.05–5 μg/ml) and CD28 mAbs (1 μg/ml) on cell proliferation were evaluated. Proliferation was measured on day 3 for CD3 mAb and on day 5 for PPD by adding [^{3}H]thymidine (NEN, Boston, MA) at 1 μCi/well during the last 16 h of culture. All cultures were set up in triplicate.

Immunoprecipitation

Cells used for immunoprecipitation were KG-1 cells, PBMCs, MACS-purified $CD14^+$ monocytes, PBMCs depleted with $CD14^+$ monocytes, MACS-purified $CD4^+$ T cells, and activated $CD4^+$ T cells. Cells (5×10^6-1×10^7) were labeled at the cell surface by lactoperoxidase-catalyzed iodination as described previously (38). Radioiodinated cells were lysed with extraction buffer (0.5% Nonidet P-40, 10 mM Tris-HCl, 0.15 M NaCl, 1 mM PMSF, and 0.02% NaN_3) for 10 min on ice. The mixture was centrifuged at $27,000 \times g$ at 4°C for 20 min, and the supernatant was collected. Immunoprecipitations were performed by incubating radiolabeled cell lysate with 10 μg of HSCA-2, DFT-1, or MOPC21 mAbs for 1 h on ice, then adding a 20 μl-packed volume of protein G-Sepharose (Amersham Pharmacia Biotech, Piscataway, NJ), and further incubating the mixture for 30 min. Immunoprecipitates were washed four times in extraction buffer and solubilized in reducing Laemmli sample buffer subjected to SDS-PAGE (7.5% gel). After fixing and drying, the gels were autoradiographed at −80°C using x-ray film. Prestained SDS-PAGE standards were obtained from Bio-Rad (Hercules, CA).

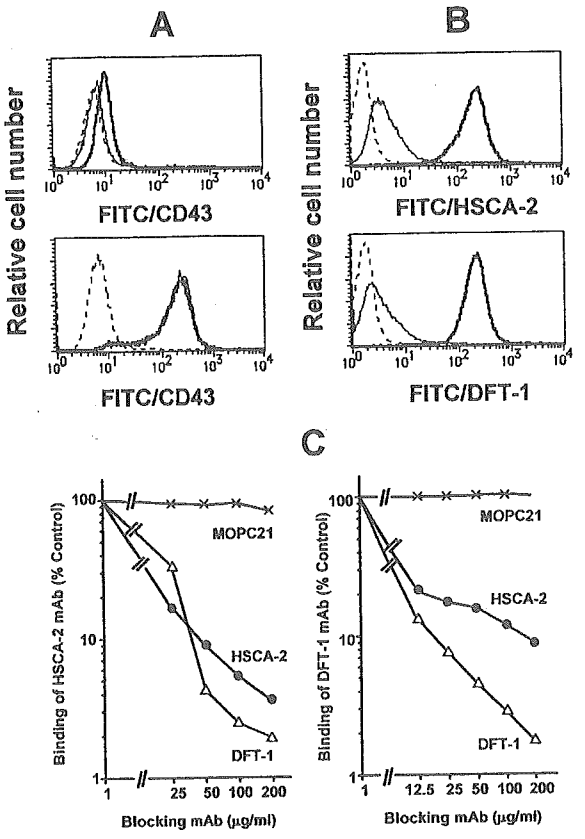

FIGURE 1. Flow cytometric analyses of CD43 expression in $CD43^+$ HeLa transfectant and KG-1 cells with HSCA-2 and DFT-1 mAbs. *A*, Direct immunofluorescence staining of mock-transfected (*upper panel*) and CD43-transfected HeLa cells (*lower panel*) with FITC-labeled HSCA-2 (thick line), DFT-1 (thin line), and control IgG1 (broken line) mAbs. *B*, Effect of neuraminidase treatment on the expression of CD43 in KG-1 cells. Nontreated (thick line) and treated (thin line) KG-1 cells were stained with FITC-labeled HSCA-2 (*upper panel*), DFT-1 (*lower panel*) mAbs. Treated cells also were stained with control IgG1 (broken line). *C*, Blocking of the binding of FITC-labeled HSCA-2 (*left*) and DFT-1 (*right*) mAbs to KG-1 cells by excess amounts of HSCA-2, DFT-1, or MOPC21 (IgG1 control) mAbs.

Results

Characterization of CD43 epitopes recognized by HSCA-2 mAb

HSCA-2 mAb resembles the reference CD43 mAb DFT-1 in binding to HeLa cells stably transfected with $CD43^+$ cDNA, but not to their mock-transfected ($CD43^-$) counterparts (Fig. 1*A*). HSCA-2 mAb also resembles the DFT-1 mAb in recognizing a neuraminidase-sensitive epitope on KG-1 cells (Fig. 1*B*). However, although the binding of HSCA-2 mAb to KG-1 cells was all but completely blocked by DFT-1 mAb, the binding of DFT-1 mAb was only ~90% blocked by HSCA-2 mAb even at the highest HSCA-2 mAb concentration (Fig. 1*C*). These findings may imply that the binding affinity of HSCA-2 mAb is lower than that of DFT-1 mAb. The HSCA-2 mAb immunoprecipitated a surface protein of ~115 kDa in KG-1 cells, whereas DFT-1 mAb immunoprecipitated both the115-kDa protein and a minor protein with a higher molecular mass of ~125 kDa (Fig. 2*A*). Immunoprecipitation and blocking experiments with another characterized CD43 mAb, 1G10, confirmed the results with the DFT-1 mAb (data not shown). These results suggest that HSCA-2 mAb reacts with a

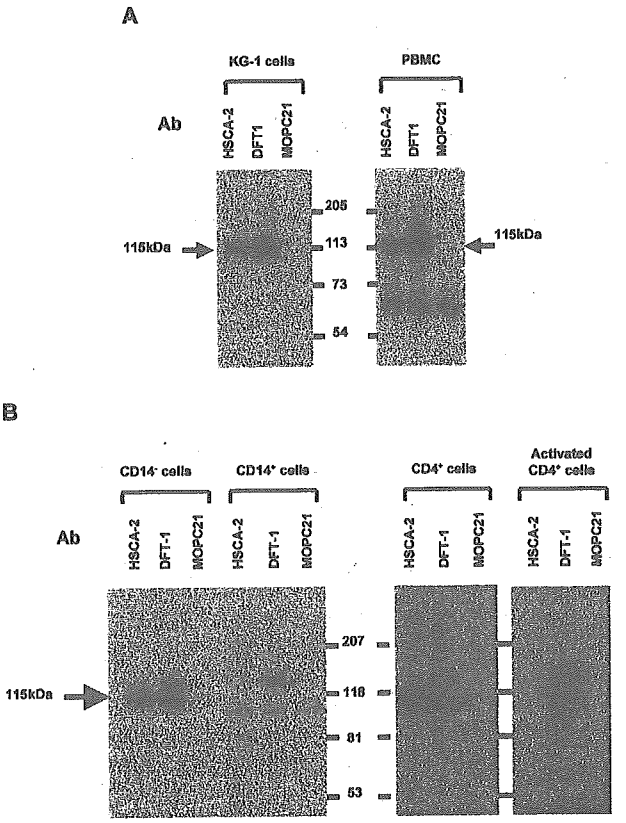

FIGURE 2. Immunoprecipitation of ^{125}I-labeled surface proteins from various types of white blood cells with HSCA-2, DFT-1, and MOPC21 (IgG1 control) mAbs. *A*, Immunoprecipitation of KG-1 cells and total PBMCs. *B*, Immunoprecipitation of $CD14^-$, $CD14^+$, $CD4^+$, and activated $CD4^+$ cells; 105-, 115-, 125-, and 135-kDa protein bands are indicated by an asterisk, arrows, open triangles, and closed triangles, respectively.

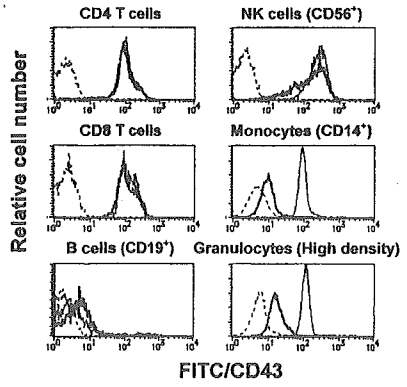

FIGURE 3. Flow cytometric analyses of CD43 expression in peripheral blood cells. For two-color analyses, PBMCs were stained with FITC-labeled HSCA-2 (thick line), DFT-1 (thin line), and control IgG1 (broken line) mAbs in combination with PE-labeled CD4, CD8, CD19, and CD56 mAbs. Monocytes and granulocytes isolated by MACS with CD14 mAb and density centrifugation, respectively, were singly stained with FITC-labeled mAbs. Results are representative of seven different donors.

sialic acid-dependent epitope on the 115-kDa CD43 glycoform in KG-1 cells, but not with its equivalent on the 125-kDa glycoform.

Expression characteristics of CD43 in normal white blood cells

The particular CD43 epitopes recognized by the HSCA-2 or DFT-1 mAb (hereafter abbreviated to CD43(HSCA-2) or CD43(DFT-1)) in normal lymphoid and myeloid cell populations were analyzed by two-color flow cytometry (Fig. 3). The CD43(HSCA-2) and CD43(DFT-1) epitopes were expressed at similar levels in $CD4^+$ and $CD8^+$ T cell populations. Neither HSCA-2 mAb nor DFT-1 mAb reacted with resting $CD19^+$ B cells, whereas they both bound reasonably strongly to either PWM-activated or EBV-transformed B cells (data not shown). The majority of $CD56^+$ NK cells expressed both CD43(HSCA-2) and CD43(DFT-1) epitopes at high levels, whereas there was relatively little of the CD43(HSCA-2) epitope in the minor subpopulation of NK cells. DFT-1 mAb was found to bind quite strongly to both purified monocytes and granulocytes, whereas binding by the HSCA-2 mAb was weak enough to be described as nonspecific, as judged by the results of immunoprecipitation analyses (see Fig. 2*B*). We did not detect any increase in the level of either CD43(HSCA-2) or CD43(DFT-1) in cultured monocytes, even after the addition of LPS (data not shown). The HSCA-2 and DFT-1 mAbs both reacted quite strongly with cord blood $CD34^+$ cells (data not shown). Two previously used CD43 mAbs, 1G10 and L10, appeared to share the cell type specificities of the DFT-1 mAb (data not shown).

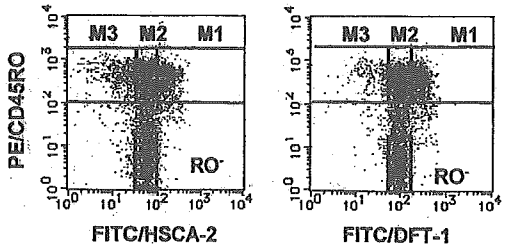

FIGURE 4. Flow cytometric analyses of CD43 expression in $CD4^+$ T cell subsets. Expression of CD43 detected by either HSCA-2 (*left*) or DFT-1 (*right*) mAbs in combination with CD45RO in $CD4^+$ T cells analyzed by triple-color immunofluorescence. Four different subsets were defined within $CD4^+$T cells: $CD45RO^+$ cells expressing higher (M1), intermediate (M2), and lower (M3) levels of CD43, and $CD45RO^-$ (RO^-) cells in each CD43 mAb. In each donor a window for the M2 subset was set in a region where the CD43 level detected by each CD43 mAb was from approximately one-half to 2-fold the mean CD43 intensity for RO^- cells. Results are representative of six donors.

The results of experiments involving immunoprecipitation of ^{125}I-labeled surface proteins from PBMCs, $CD14^-$ lymphoid cells, and $CD4^+$ T cells with CD43 mAbs revealed that the HSCA-2 mAb recognizes only 115-kDa proteins, and whereas the DFT-1 mAb also reacts with 115-kDa proteins it can interact with a second minor, but higher molecular mass (~125 kDa), protein as well (Fig. 2); these findings mirror our previous findings with KG-1 cells (see above). Other findings include the fact that HSCA-2 mAb failed to immunoprecipitate any specific proteins from $CD14^+$ monocytes, unlike the DFT-1 mAb, which reacted with a 135-kDa protein (Fig. 2*B*). In tests with activated $CD4^+$ T cells, the DFT-1 mAb immunoprecipitated both the 135-kDa protein and a minor protein with lower molecular mass of 105 kDa, unlike the HSCA-2 mAb, which did not react with proteins of either of these sizes (Fig. 2*B*). Both the HSCA-2 and DFT-1 mAbs appeared to specifically immunoprecipitate several common, low molecular mass (25- to 40-kDa) proteins in activated $CD4^+$ T cells (data not shown).

Expression characteristics of CD43 in $CD4^+$ memory T cells

As shown in Fig. 4 (*left*), the $CD4^+CD45RO^+$ cell population can be divided into three distinct subsets (M1, M2, and M3) on the basis of their CD43(HSCA-2) expression levels; this confirms our previous findings (31). We therefore tried to define the same three subsets on the basis of their CD43(DFT-1) expression levels (Fig. 4, *right*); interestingly, the proportions of the M1 subset detected with the DFT-1 and HSCA-2 mAbs were not significantly different (Table I), whereas the proportion of the M2 subset defined by the DFT-1 mAb was significantly larger when defined by HSCA-2 mAb, and the proportion of the M3 subset defined by the DFT-1 mAb was significantly smaller than when defined by HSCA-2 mAb. We observed similar subset percentages when the 1G10 and L10 mAbs were used in place of the DFT-1 mAb (Table I). These results indicate that the low levels of CD43(HSCA-2) expression that typify the M3 population do not affect the ability of M3 cells to express other CD43 epitopes.

Accessory functions of CD43 in recall responses of $CD4^+$ memory T cells

To analyze possible accessory functions of CD43(HSCA-2) in memory T cells, we first examined the effects of exposure to HSCA-2 mAb on the recall Ag-induced proliferation of total PBMCs in culture. As shown in Fig. 5, HSCA-2 mAb seemed to

Table I. *CD4 memory T cell subsets defined by four different CD43 mAbs*

CD43 mAb	Subsets (% in total $CD4^+$ T cells[a])		
	M1	M2	M3
HSCA-2	19.9 ± 4.4[b]	21.8 ± 8.0	5.7 ± 3.0
DFT-1	19.0 ± 3.7	25.3 ± 9.4[c]	3.0 ± 1.4[c]
L10	20.5 ± 4.3	23.6 ± 8.7[c]	2.6 ± 1.4[c]
1G10	19.0 ± 4.1	24.5 ± 8.2[c]	2.8 ± 1.8[c]

[a] The percentage of each subset in total $CD4^+$ T cells was determined by three-color flow cytometry, as shown in Fig. 4*A*.
[b] Average ± SD (n = 6)
[c] Value was significantly larger or smaller than that of HSCA-2 mAb by Wilcoxon signed rank test ($p < 0.05$).

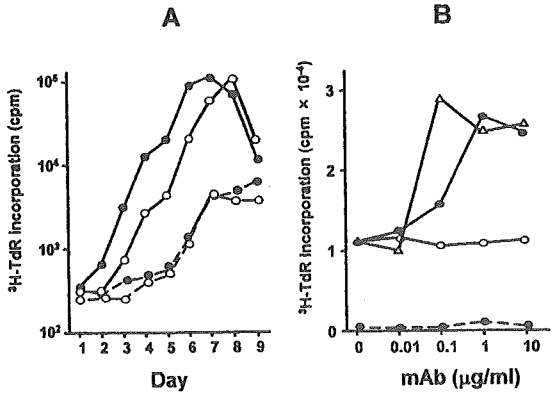

FIGURE 5. Acceleration of proliferative responses of PBMCs to PPD by stimulation with CD43 mAbs. *A*, Time courses of PPD responses. PBMCs were stimulated with (solid line) or without (broken line) PPD (5 μg/ml) in the presence (●) or the absence (○) of HSCA-2 mAb (5 μg/ml). *B*, Dose responses of CD43 mAbs. PBMCs were stimulated with (solid line) or without (broken line) PPD (5 μg/ml) in the presence of HSCA-2 (●), DFT-1 (△), and MOPC21 (○) at the various concentrations. Proliferation was measured on day 5 by adding [^{3}H]thymidine during the last 16 h of culture. Results are representative of five donors.

dose-dependently accelerate the proliferation of PPD Ag-stimulated PBMCs, but had no comparable effect on their proliferation in the absence of PPD. The three traditionally used anti-CD43 mAbs (DFT-1 (Fig. 5*B*), and 1G10 and L10 (data not shown)) also proved at least as effective as the HSCA-2 mAb in accelerating PPD-stimulated proliferation of PBMCs. As the majority of PPD-reactive cells appear to be CD4$^+$ T cells (data not shown), we examined the effects of the addition of a combination of HSCA-2 mAb and CD28 mAb on the responses of MACS-purified CD4$^+$ T cells in the presence of autologous monocytes (Fig. 6). The CD28 mAb that we chose to use in this experiment was the CD28.2 clone, which is capable of strongly costimulating polyclonal T cell responses to plastic- or monocyte-bound CD3 mAb, but (if anything) inhibits Ag-specific responses (39). Thus, whereas HSCA-2 mAb led to a significantly enhanced PPD response in CD4$^+$ T cells, the addition of CD28 mAb led to it being slightly inhibited. We also examined the effect of the HSCA-2 mAb on the TT-dependent proliferative response of CD4$^+$ T cells and found that it had an enhancing effect (Fig. 6).

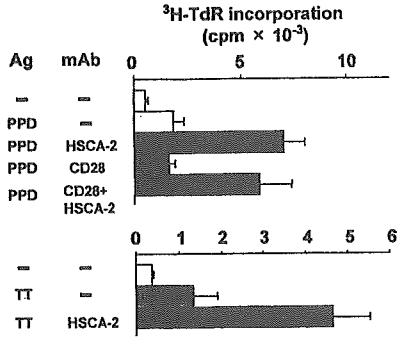

FIGURE 6. Effects of HSCA-2 and CD28 mAbs on the proliferative responses of CD4 T cells to recall Ags. MACS-purified CD4 T cells were stimulated with PPD or TT in the presence of autologous CD14$^+$ APC. HSCA-2 (5 μg/ml) and/or CD28 (1 μg/ml) mAbs were added to the culture. Proliferation was measured on day 5 (PPD) or day 7 (TT) by adding [^{3}H]thymidine during the last 16 h of culture. Results were expressed as the mean cpm ± SD and are representative of three donors.

Next we examined the effects of the addition of CD28 and HSCA-2 mAbs on recall responses in each of the three CD4$^+$ memory T cell subsets as defined by their separation in a cell sorter on the basis of their CD43(HSCA-2) expression levels (Fig. 4). As shown in Fig. 7*A*, only the M1 subset cells appeared to be capable of responding to PPD; this confirms our previous findings (31). The results of our experiments with the M1 subset mirrored our findings with unseparated CD4$^+$ T cell populations, in that the PPD response of M1 subset cells was significantly and dose-dependently enhanced by the addition of HSCA-2 mAb (Fig. 7, *B* and *C*), but was inhibited, rather than enhanced, in the presence of the CD28 mAb (Fig. 7*A*). The PPD responses of the M2 and M3 subset cells were virtually unaffected by the addition of the HSCA-2 mAb (Fig. 7, *B* and *C*). This did not surprise us, given that the M2 and M3 subsets appeared to contain a relatively very

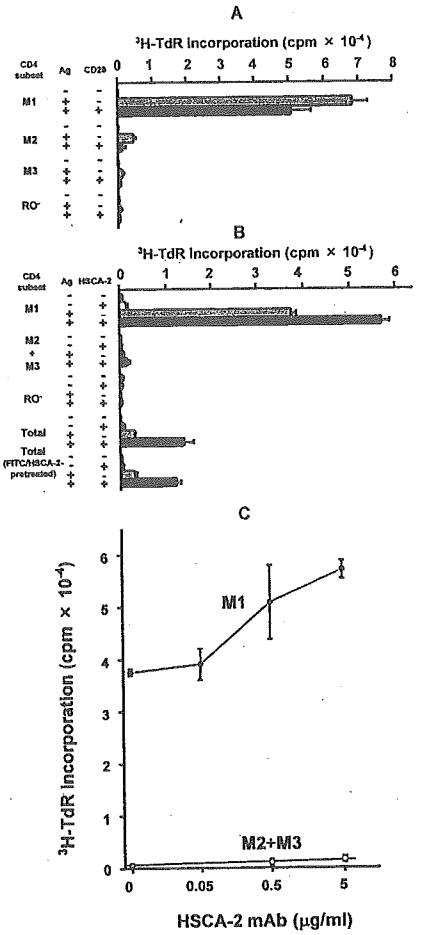

FIGURE 7. Effects of CD28 and HSCA-2 mAbs on the proliferative responses of CD4 T cell subsets to PPD. *A–C*, MACS-purified CD4$^+$ T cells were stained with FITC-HSCA-2 and PE-CD45RO mAbs (see Fig. 4*A*, *left*) and thereafter sorted by FACS into the indicated subsets. Each subset cells and total CD4$^+$ T cells were stimulated with PPD in the presence of autologous CD14$^+$ APC. CD28 (1 μg/ml; *A*) or HSCA-2 (5 μg/ml; *B*) mAbs were added to the culture. Total CD4$^+$ T cells pretreated with FITC-HSCA-2 mAb also were examined for possible effects of immunofluorescence staining with HSCA-2 mAb on the PPD response (*B*). M2+M3, Cell populations sorted by gating the combined region of the M2 and M3 subsets (Fig. 4*A*, *left*). Dose responses of HSCA-2 mAb for M1 subset cells and a combined cell population of M2 and M3 subsets were examined (*C*). Proliferation was measured on day 5 by adding [^{3}H]thymidine during the last 16 h of culture. Results were expressed as the mean cpm ± SD and are representative of three donors.

small PPD-reactive precursor component (31). The stimulatory effect of the FITC-HSCA-2 mAb that remains attached to cells after its use in the course of their separation was negligible, given that the pretreatment of unseparated $CD4^+$ T cells with FITC-HSCA-2 mAb did not significantly alter their subsequent response to PPD, whereas addition of the mAb to cultures of both FITC-HSCA-2 mAb-pretreated and nontreated $CD4^+$ T cells increased their responses to PPD to very much the same extent (Fig. 7*B*). Taken together, the above results indicate that CD43(HSCA-2) is capable of acting as an accessory molecule in the Ag-specific recall response of mature $CD4^+$ memory T cells.

Synergistic effects between CD43 and CD28 mAbs in polyclonal response

To determine whether CD43(HSCA-2) can play an accessory role in the polyclonal activation of T cells, we examined the possible effects of the HSCA-2 mAb on the proliferative response of $CD4^+$ T cells to monocyte-bound CD3 mAb (Fig. 8). We found that the HSCA-2 mAb did have an effect, but that it was only marginally costimulatory at lower (0.001–0.1 μg/ml) CD3 mAb concentrations and that its effectiveness disappeared at the highest concentration tested (1 μg/ml). Interestingly, the results shown in Fig. 8*A* provide convincing evidence that the CD28/HSCA-2 mAb combination had a synergistic effect on the CD3 mAb-mediated polyclonal response (Fig. 8*A*). A similar synergistic effect on the CD3-mediated response was observed when the mAbs involved were DFT-1 and CD28 (data not shown).

Cells of two of the three $CD4^+$ memory T cell subsets (M1 and M2) responded strongly to monocyte-bound CD3 mAb, whereas M3 subset cells did not (Fig. 8*B*). These findings are in agreement with those in our original report (31). The HSCA-2 mAb was almost as effective as CD28 mAb in their enhancement of polyclonal responses in M1 and M2 subset cells, but had no such effect in M3 subset cells. There were marginal synergistic effects on polyclonal responses when M1 and M2 subset cells were cotreated with the HSCA-2 and CD28 mAbs, although a much more obvious synergistic effect became evident when we used RO^- naive subset cells instead.

When the Fab portion of the HSCA-2 mAb was used instead of intact Ab, we could see no indication of either an enhanced PPD-mediated stimulatory response or a synergistic interaction involving the CD28 mAb and CD3 mAb polyclonal responses (data not shown).

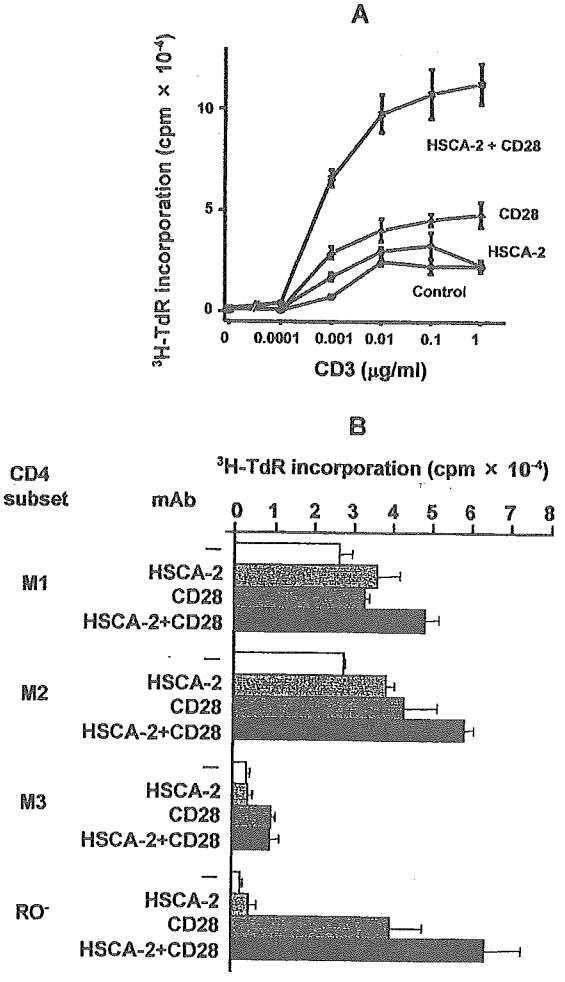

FIGURE 8. Synergistic effects of HSCA-2 and CD28 mAbs on the proliferative responses of $CD4^+$ T cells to monocyte-bound CD3 mAb. Total $CD4^+$ T cells (*A*) and $CD4^+$ T cell subset cells (*B*) were stimulated with various concentrations (*A*) or 0.1 μg/ml (*B*) of CD3 mAb in the presence of autologous $CD14^+$ monocytes. The effects of HSCA-2 (5 μg/ml) and CD28 (1 μg/ml) mAbs on the CD3 responses were tested by single or combined use of these mAbs. Proliferation was measured on day 3 by adding [^{3}H]thymidine during the last 16 h of culture. Results were expressed as the mean cpm ± SD and are representative of three donors.

Discussion

HSCA-2 mAb specifically recognizes a neuraminidase-sensitive epitope on the low molecular mass (115-kDa) glycoform of the CD43 molecule that is predominantly expressed in lymphoid cells, including resting T and NK cells. By contrast, all previously described CD43 mAbs (including the DFT-1 mAb) react strongly or even very strongly with a larger (135-kDa) CD43 glycoform that is expressed in myeloid cells such as monocytes and granulocytes. Importantly, the HSCA-2 mAb does not appear to recognize the 135-kDa glycoform and hence binds only marginally, if at all, to myeloid cells; it also does not immunoprecipitate a third high molecular mass (125-kDa) CD43 protein that is recognized by the DFT-1mAb in both KG-1 and $CD4^+$ T cells. Taken together, these findings suggest that the HSCA-2 mAb is specific for a novel glycoepitope on the 115-kDa glycoform of CD43.

Interestingly, HSCA-2 mAb differs from all pre-existing CD43 mAbs in being unable to recognize the high molecular mass CD43 glycoform (135 kDa) that is present on activated $CD4^+$ T cells. Thus, the 135-kDa CD43 glycoform consists of a more fully glycosylated version that is generated in the course of the increase in molecular mass of the 115-kDa CD43 glycoform that occurs during T cell activation (5, 7); it is possible that the HSCA-2 glycoepitope is either lost or masked in the course of this glycosyl modification process. As the molecular mass of the CD43 polypeptide is ~40 kDa, the 25- to 40-kDa proteins recognized by HSCA-2 mAb in activated T cells could well be degradation forms of CD43, and we have even observed what appeared to be the gradual disappearance of CD43(HSCA-2) epitopes from a subpopulation of activated $CD4^+CD45RO^+$ T cells (manuscript in preparation).

We noticed that there were significant differences in the distribution of the CD4 memory T cell subsets depending upon which of the available CD43 mAbs was used in their separation. Thus, for example, the percentages of M2 subset cells that we observed in separations achieved using the HSCA-2 mAb were significantly smaller than those observed in separations using any of the other available mAbs. In the case of the M3 subsets, the percentages were larger with the HSCA-2 mAb than with any of the others. These CD43 mAb-dependent differences in subset distributions

may correspond to differences in such subset cell functions as memory vs anergy, but we have yet to explore this possibility in any detail.

In this report we show that HSCA-2 and certain other CD43 mAbs are capable of accelerating both the recall Ag-induced and CD3 mAb-induced proliferation of CD4 memory T cells. There are previous reports indicating that CD43 molecules may also have accessory involvements in T cell activation, such as, for example, in mice, where CD43 mAb appears to costimulate T cell activation during treatment with plastic-bound CD3 mAb and alloantigens (17, 40). In humans, however, there does not appear to be any evidence of CD43 mAb being involved in a costimulatory capacity in the polyclonal activation of T cells (41). In situations involving Ag-specific responses, there is one report that CD43 is necessary for the production of IL-2 in HLA class II-specific human hybridoma T cells (42), but it is important to note that the experimental system used to obtain these data was an unusually artificial one. There are, however, several publications in which it is claimed that a number of CD43 mAbs can stimulate Ag-independent human T cell proliferation in a multicomponent test system that requires the presence of CD43-stimulated monocytes (43–46). Thus, the results described in this study appear to provide the first evidence that T cell-determined CD43 may help to stimulate the Ag-specific proliferative responses of freshly isolated T cells in humans. In the case of our new mAb (HSCA-2), we can exclude any involvement of CD43-mediated monocyte stimulation in T cell activation. The reason why HSCA-2 mAb differs from all previously used CD43 mAbs in this important way is that it appears to lack reactivity to the 135-kDa CD43 glycoform expressed in monocytes.

Given the above consideration, it seems reasonable to assume that CD43 plays a part in some of the cell signaling events that are likely to be involved in memory T cell activation. Up-regulated expression of CD43 in M1 subset cells may cause an increase in activation signaling in concert with other up-regulated costimulatory molecules such as CD28 (31). Our observation that CD43 and CD28 mAbs act synergistically to stimulate the polyclonal response of CD4$^+$ T cells to anti-CD3 mAb may indicate that both CD43 and CD28 have an accessory signaling role in the induction of the polyclonal response. It has previously been reported that T cell activation through CD43 cross-linking in humans induces serine phosphorylation of Cbl proteins and tyrosine phosphorylation of Vav (19, 20). It has also been reported that one of the CD28-determined costimulatory signaling processes is mediated by tyrosine phosphorylation of Vav1, which is, in turn, negatively regulated by Cbl-b (47–49). Thus, although the precise molecular mechanisms underlying the costimulatory effects of CD43 remain to be determined, it is possible that both CD28 and CD43 are capable of synergistically enhancing the activation of CD4$^+$ memory T cells by a mechanism involving the common signaling pathway.

Acknowledgments

We grateful to Dr. Donald MacPhee for his valuable suggestions, to Mika Yamaoka for her excellent assistance with FACS analysis, and to Mika Yonezawa and Jeffrey Hart for manuscript preparation.

References

1. Remold-O'Donnell, E. 1995. CD43 cluster report. In *Leucocyte Typing.* Vol. V: *White Cell Differentiation Antigens.* S. F. Schlossman, L. Boumsell, W. Gilks, J. M. Harlan, T. Kishimoto, C. Morimoto, J. Ritz, S. Shaw, R. Silverstein, T. Springer, et al., eds. Oxford University Press, New York, p. 1697.
2. Rosenstein, Y., A. Santana, and G. Pedraza-Alva. 1999. CD43, a molecule with multiple functions. *Immunol. Res. 20:89.*
3. Cyster, J. G., D. M. Shotton, and A. F. Williams. 1991. The dimensions of the T lymphocyte glycoprotein leukosialin and identification of linear protein epitopes that can be modified by glycosylation. *EMBO J. 10:893.*
4. Carlsson, S. R., H. Sasaki, and M. Fukuda. 1986. Structural variations of *O*-linked oligosaccharides present in leukosialin isolated from erythroid, myeloid, and T-lymphoid cell lines. *J. Biol. Chem. 261:12787.*
5. Piller, F., F. Le Deist, K. I. Weinberg, R. Parkman, and M. Fukuda. 1991. Altered *O*-glycan synthesis in lymphocytes from patients with Wiskott-Aldrich syndrome. *J. Exp. Med. 173:1501.*
6. Jones, A. T., B. Federsppiel, L. G. Ellies, M. J. Williams, R. Burgener, V. Duronio, C. A. Smith, F. Takei, and H. J. Ziltener. 1994. Characterization of the activation-associated isoform of CD43 on murine T lymphocytes. *J. Immunol. 153:3426.*
7. Piller, F., V. Piller, R. I. Fox, and M. Fukuda. 1988. Human T-lymphocyte activation is associated with changes in *O*-glycan biosynthesis. *J. Biol. Chem. 263:15146.*
8. Harrington, L. E., M. Galvan, L. G. Baum, J. D. Altman, and R. Ahmed. 2000. Differentiating between memory and effector CD8 T cells by altered expression of cell surface *O*-glycans. *J. Exp. Med. 191:1241.*
9. Onami, T. M., L. E. Harrington, M. A. Williams, M. Galvan, C. P. Larsen, T. C. Pearson, N. Manjunath, L. G. Baum, B. D. Pearce, and R. Ahmed. 2002. Dynamic regulation of T cell immunity by CD43. *J. Immunol. 168:6022.*
10. Ostberg, J. R., R. K. Barth, and J. G. Frelinger. 1998. The Roman god Janus: a paradigm for the function of CD43. *Immunol. Today 19:546.*
11. Manjunath, N., M. Correa, M. Ardman, and B. Ardman. 1995. Negative regulation of T-cell adhesion and activation by CD43. *Nature 377:535.*
12. Stockton, B. M., G. Cheng, N. Manjunath, B. Ardman, and U. H. von Andrian. 1998. Negative regulation of T cell homing by CD43. *Immunity 8:373.*
13. McEvoy, L. M., H. Sun, J. G. Frelinger, and E. C. Butcher. 1997. Anti-CD43 inhibition of T cell homing. *J. Exp. Med. 185:1493.*
14. Woodman, R. C., B. Johnston, M. J. Hickey, D. Teoh, P. Reinhardt, B. Y. Poon, and P. Kubes. 1998. The functional paradox of CD43 in leukocyte recruitment: a study using CD43-deficient mice. *J. Exp. Med. 188:2181.*
15. He, Y. W., and M. J. Bevan. 1999. High level expression of CD43 inhibits T cell receptor/CD3-mediated apoptosis. *J. Exp. Med. 190:1903.*
16. Brown, T. J., W. W. Shuford, W. C. Wang, S. G. Nadler, T. S. Bailey, H. Marquardt, and R. S. Mittler. 1996. Characterization of a CD43/leukosialin-mediated pathway for inducing apoptosis in human T-lymphoblastoid cells. *J. Biol. Chem. 271:27686.*
17. Sperling, A. I., J. M. Green, R. L. Mosley, P. L. Smith, R. J. DiPaolo, J. R. Klein, J. A. Bluestone, and C. B. Thompson. 1995. CD43 is a murine T cell costimulatory receptor that functions independently of CD28. *J. Exp. Med. 182:139.*
18. Pedraza-Alva, G., L. B. Merida, S. J. Burakoff, and Y. Rosenstein. 1996. CD43-specific activation of T cells induces association of CD43 to Fyn kinase. *J. Biol. Chem. 271:27564.*
19. Pedraza-Alva, G., L. B. Merida, S. J. Burakoff, and Y. Rosenstein. 1998. T cell activation through the CD43 molecule leads to Vav tyrosine phosphorylation and mitogen-activated protein kinase pathway activation. *J. Biol. Chem. 273:14218.*
20. Pedraza-Alva, G., S. Sawasdikosol, Y. C. Liu, L. B. Merida, M. E. Cruz-Munoz, F. Oceguera-Yanez, S. J. Burakoff, and Y. Rosenstein. 2001. Regulation of Cbl molecular interactions by the co-receptor molecule CD43 in human T cells. *J. Biol. Chem. 276:729.*
21. Thurman, E. C., J. Walker, S. Jayaraman, N. Manjunath, B. Ardman, and J. M. Green. 1998. Regulation of in vitro and in vivo T cell activation by CD43. *Int. Immunol. 10:691.*
22. Carlow, D. A., S. Y. Corbel, and H. J. Ziltener. 2001. Absence of CD43 fails to alter T cell development and responsiveness. *J. Immunol. 166:256.*
23. Allenspach, E. J., P. Cullinan, J. Tong, Q. Tang, A. G. Tesciuba, J. L. Cannon, S. M. Takahashi, R. Morgan, J. K. Burkhardt, and A. I. Sperling. 2001. ERM-dependent movement of CD43 defines a novel protein complex distal to the immunological synapse. *Immunity 15:739.*
24. Delon, J., K. Kaibuchi, and R. N. Germain. 2001. Exclusion of CD43 from the immunological synapse is mediated by phosphorylation-regulated relocation of the cytoskeletal adaptor moesin. *Immunity 15:691.*
25. Shaw, A. S. 2001. FERMing up the synapse. *Immunity 15:683.*
26. Stoll, S., J. Delon, T. M. Brotz, and R. N. Germain. 2002. Dynamic imaging of T cell-dendritic cell interactions in lymph nodes. *Science 296:1873.*
27. Cullinan, P., A. I. Sperling, and J. K. Burkhardt. 2002. The distal pole complex: a novel membrane domain distal to the immunological synapse. *Immunol. Rev. 189:111.*
28. Savage, N. D., S. L. Kimzey, S. K. Bromley, K. G. Johnson, M. L. Dustin, and J. M. Green. 2002. Polar redistribution of the sialoglycoprotein CD43: implications for T cell function. *J. Immunol. 168:3740.*
29. Youseffi-Etemad, R., and B. Axelsson. 1996. Parallel pattern of expression of CD43 and of LFA-1 on the CD45RA$^+$ (naive) and CD45RO$^+$ (memory) subsets of human CD4$^+$ and CD8$^+$ cells: correlation with the aggregative response of the cells to CD43 monoclonal antibodies. *Immunology 87:439.*
30. Mukasa, R., T. Homma, T. Ohtsuki, O. Hosono, A. Souta, T. Kitamura, M. Fukuda, S. Watanabe, and C. Morimoto. 1999. Core 2-containing *O*-glycans on CD43 are preferentially expressed in the memory subset of human CD4 T cells. *Int. Immunol. 11:259.*
31. Ohara, T., K. Koyama, Y. Kusunoki, T. Hayashi, N. Tsuyama, Y. Kubo, and S. Kyoizumi. 2002. Memory functions and death proneness in three CD4$^+$CD45RO$^+$ human T cell subsets. *J. Immunol. 169:39.*
32. Sallusto, F., D. Lenig, R. Forster, M. Lipp, and A. Lanzavecchia. 1999. Two subsets of memory T lymphocytes with distinct homing potentials and effector functions. *Nature 401:708.*
33. Kyoizumi, S., M. Akiyama, N. Kouno, K. Kobuke, M. Hakoda, S. L. Jones, and M. Yamakido. 1985. Monoclonal antibodies to human squamous cell carcinoma of the lung and their application to tumor diagnosis. *Cancer Res. 45:3274.*

34. Andrew, S. M., and J. Titus. 1996. Fragmentation of immunogloblin G. In *Current Protocols in Immunology.* J. E. Coligan, A. M. Kruisbeek, D. H. Margulies, E. M. Shevach, and W. Strober, eds. John Wiley & Sons, New York and London, p. 2. 10.
35. Nunes, J., S. Klasen, M. Ragueneau, C. Pavon, D. Couez, C. Mawas, M. Bagnasco, and D. Olive. 1993. CD28 mAbs with distinct binding properties differ in their ability to induce T cell activation: analysis of early and late activation events. *Int. Immunol. 5:311.*
36. Remold-O'Donnell, E., D. M. Kenney, R. Parkman, L. Cairns, B. Savage, and F. S. Rosen. 1984. Characterization of a human lymphocyte surface sialoglycoprotein that is defective in Wiskott-Aldrich syndrome. *J. Exp. Med. 159:1705.*
37. Horejsi, V., and H. Stockinger. 1997. CD43 workshop panel report. In *Leucocyte Typing*, Vol. VI: *White Cell Differentiation Antigens.* T. Kishimoto, H. Kikutani, A. E. G. Kr. von dem Borne, S. M. Goyert, D. Y. Mason, M. Miyasaka, L. Moretta, K. Okumura, S. Shaw, T. A. Springer, et al., eds. Garland, New York and London, p. 494.
38. Kyoizumi, S., M. Akiyama, Y. Hirai, Y. Kusunoki, K. Tanabe, and S. Umeki. 1990. Spontaneous loss and alteration of antigen receptor expression in mature $CD4^+$ T cells. *J. Exp. Med. 171:1981.*
39. Olive, D., C. Cerdan, R. Costello, I. Sielleur, M. Ragueneau, F. Pages, S. Klasen, J. Nunes, and J. Imbert. 1995. CD28 and CTLA-4 cluster report. In *Leucocyte Typing*, Vol. V: *White Cell Differentiation Antigens.* S. F. Schlossman, L. Boumsell, W. Gilks, J. M. Harlan, T. Kishimoto, C. Morimoto, J. Ritz, S. Shaw, R. Silverstein, T. Springer, et al., ed. Oxford University Press, New York, p. 360.
40. Walker, J., and J. M. Green. 1999. Structural requirements for CD43 function. *J. Immunol. 162:4109.*
41. Tkaczuk, J., T. Al Saati, I. Escargueil-Blanc, A. Salvayre, V. Horejsi, M. Durand, C. de Preval, E. Ohayon, G. Delsol, and M. Abbal. 1999. The CBF.78 monoclonal antibody to human sialophorin has distinct properties giving new insights into the CD43 marker and its activation pathway. *Tissue Antigens 54:1.*
42. Park, J. K., Y. J. Rosenstein, E. Remold-O'Donnell, B. E. Bierer, F. S. Rosen, and S. J. Burakoff. 1991. Enhancement of T-cell activation by the CD43 molecule whose expression is defective in Wiskott-Aldrich syndrome. *Nature 350:706.*
43. Mentzer, S. J., E. Remold-O'Donnell, M. A. Crimmins, B. E. Bierer, F. S. Rosen, and S. J. Burakoff. 1987. Sialophorin, a surface sialoglycoprotein defective in the Wiskott-Aldrich syndrome, is involved in human T lymphocyte proliferation. *J. Exp. Med. 165:1383.*
44. Axelsson, B., R. Youseffi-Etemad, S. Hammarstrom, and P. Perlmann. 1988. Induction of aggregation and enhancement of proliferation and IL-2 secretion in human T cells by antibodies to CD43. *J. Immunol. 141:2912.*
45. Nong, Y. H., E. Remold-O'Donnell, T. W. LeBien, and H. G. Remold. 1989. A monoclonal antibody to sialophorin (CD43) induces homotypic adhesion and activation of human monocytes. *J. Exp. Med. 170:259.*
46. Alvarado, M., C. Klassen, J. Cerny, V. Horejsi, and R. E. Schmidt. 1995. MEM-59 monoclonal antibody detects a CD43 epitope involved in lymphocyte activation. *Eur. J. Immunol. 25:1051.*
47. Chiang, Y. J., H. K. Kole, K. Brown, M. Naramura, S. Fukuhara, R. J. Hu, I. K. Jang, J. S. Gutkind, E. Shevach, and H. Gu. 2000. Cbl-b regulates the CD28 dependence of T-cell activation. *Nature 403:216.*
48. Bachmaier, K., C. Krawczyk, I. Kozieradzki, Y. Y. Kong, T. Sasaki, A. Oliveira-dos-Santos, S. Mariathasan, D. Bouchard, A. Wakeham, A. Itie, et al. 2000. Negative regulation of lymphocyte activation and autoimmunity by the molecular adaptor Cbl-b. *Nature 403:211.*
49. Krawczyk, C., K. Bachmaier, T. Sasaki, G. R. Jones, B. S. Snapper, D. Bouchard, I. Kozieradzki, S. P. Ohashi, W. F. Alt, and M. J. Penninger. 2000. Cbl-b is a negative regulator of receptor clustering and raft aggregation in T cells. *Immunity 13:463.*

RADIATION RESEARCH 161, 290–298 (2004)
0033-7587/04 $15.00

Decreases in Percentages of Naïve CD4 and CD8 T Cells and Increases in Percentages of Memory CD8 T-Cell Subsets in the Peripheral Blood Lymphocyte Populations of A-Bomb Survivors

Mika Yamaoka,[a] Yoichiro Kusunoki,[a,1] Fumiyoshi Kasagi,[b] Tomonori Hayashi,[a] Kei Nakachi[a] and Seishi Kyoizumi[a]

Departments of [a] Radiobiology/Molecular Epidemiology and [b] Epidemiology, Radiation Effects Research Foundation, Hiroshima, Japan

Yamaoka, M., Kusunoki, Y., Kasagi, F., Hayashi, T., Nakachi, K. and Kyoizumi, S. Decreases in Percentages of Naïve CD4 and CD8 T Cells and Increases in Percentages of Memory CD8 T-Cell Subsets in the Peripheral Blood Lymphocyte Populations of A-Bomb Survivors. *Radiat. Res.* 161, 290–298 (2004).

Our previous studies have revealed a clear dose-dependent decrease in the percentage of naïve CD4 T cells that are phenotypically CD45RA$^+$ in PBL among A-bomb survivors. However, whether there is a similar radiation effect on CD8 T cells has remained undetermined because of the unreliability of CD45 isoforms as markers of naïve and memory subsets among the CD8 T-cell population. In the present study, we used double labeling with CD45RO and CD62L for reliable identification of naïve and memory cell subsets in both CD4 and CD8 T-cell populations among 533 Hiroshima A-bomb survivors. Statistically significant dose-dependent decreases in the percentages of CD45RO$^-$/CD62L$^+$ naïve cells were found in the CD8 T-cell population as well as in the CD4 T-cell population. Furthermore, the percentages of CD45RO$^+$/CD62L$^+$ and CD45RO$^+$/CD62L$^-$ memory T cells were found to increase significantly with increasing radiation dose in the CD8 T-cell population but not in the CD4 T-cell population. These results suggest that the prior A-bomb exposure has induced long-lasting deficits in both naïve CD4 and CD8 T-cell populations along with increased proportions of these particular subsets of the memory CD8 T-cell population. © 2004 by Radiation Research Society

INTRODUCTION

T-cell homeostasis is achieved by the balance between renewal and death among naïve and memory T cells, and maintenance of both naïve and memory T-cell pools is important for the body to protect itself against intrusions by pathogens (*1*). Exposure to radiation is thought to affect T-cell homeostasis, but little is known about the effects of radiation on the naïve and memory T-cell pools and their relationship to disease development (*2–4*), even though increased risks of various diseases including infectious (*5*) and autoimmune diseases (*6*) are still observed among A-bomb survivors. Our study therefore aimed to clarify whether the previous radiation exposure might have brought about a perturbation of T-cell homeostasis involving maintenance of normal-sized pools of both naïve and memory T cells.

Our previous studies clearly indicated that the percentages of CD4 (helper) T cells, especially those of CD45RA$^+$ (naïve) CD4 T cells, decreased in the PBL of A-bomb survivors; the decrease depended on the radiation dose (*3, 7*). The radiation sensitivity of CD4 and CD8 (cytotoxic) T cells *ex vivo* is approximately equal (*8*). In addition, the majority of CD4 and CD8 T cells are produced in the thymus by the same precursor thymocytes, CD4$^+$/CD8$^+$ cells (*9*). Thus it could be assumed that A-bomb radiation would induce similar damage to peripheral naïve CD4 and CD8 T-cell populations and that the recovery of these T-cell populations would be very similar. However, the question still remained as to the long-term effects of radiation on the recovery of naïve CD8 T-cell populations because of the unreliability of expression of CD45 isoform expression for markers of naïve CD8 T-cell populations. Several studies have proven that the CD45RA$^+$ (i.e. CD45RO$^-$) fraction of the CD8 T-cell population contains some cells that do not express the lymph node homing receptor, CD62L (L-selectin), and that these cells exhibit effector T-cell functions (*10–14*). Further indications from these studies are that naïve CD8 T-cell populations the CD45RA$^+$(CD45RO$^-$) cell fraction can be separated precisely by analyzing their CD62L expression status. In the present study, we conducted three-color flow cytometry using a combination of CD8, CD45RO and CD62L monoclonal antibodies (mAbs) to specifically enumerate the naïve and memory CD8 T-cell populations of A-bomb survivors. The percentages of CD45RO$^-$/CD62L$^+$ (naïve) CD8 T cells were found to decrease dose-dependently in the PBL of the survivors, indicating that the naïve T-cell pools are poorly maintained not only in the CD4 but also in the CD8 T-cell populations

[1] Address for correspondence: Department of Radiobiology/Molecular Epidemiology, Radiation Effects Research Foundation, 5-2 Hijiyama Park, Minami-ku, Hiroshima, 732-0815 Japan; e-mail: ykusunok@rerf.or.jp.

TABLE 1
Characterization of Study Population

	Age (years)[b]								
	<60		60–69		70–79		80+		
Dose (Gy)	Male	Female	Male	Female	Male	Female	Male	Female	Total
<0.005[a]	11	11	23	16	20	41	12	19	153
0.005–0.5	5	5	10	21	23	28	18	20	130
0.5–1.0	9	6	15	25	23	29	7	12	126
1.0–4.0	13	9	15	21	23	26	5	12	124
Total	38	31	63	83	89	124	42	63	533

[a] Individuals in this dose category were exposed at distances in excess of 3 km from the hypocenter and hence received doses that are functionally equivalent to zero.

[b] Age at the time of the examinations, which were conducted between September 2000 and February 2003.

of A-bomb survivors. Flow cytometry using CD62L marker not only allowed precise detection of naïve T cells but also enabled us to determine the percentages of memory T-cell subpopulations in PBL of A-bomb survivors, demonstrating dose-dependent increases in the percentages of $CD45RO^+/CD62L^+$ and $CD45RO^+/CD62L^-$ memory CD8 T cells.

MATERIALS AND METHODS

Study Population

Blood samples were obtained from individual members of an A-bomb survivor cohort in which 1,280 survivors, distributed almost equally by age, gender and radiation dose, had been selected from Hiroshima participants in the Adult Health Study (AHS) at the Radiation Effects Research Foundation (RERF) in 1992 (*3*). The selected study population consists of Hiroshima survivors who were exposed to significant radiation doses of 0.005 Gy or more because of their location within 2 km of the hypocenter plus a second group whose exposures were at distances in excess of 3 km from the hypocenter and as a result would have received less than 0.005 Gy (i.e. would have been exposed to doses that are indistinguishable from background). The latter group of distally exposed survivors includes the most appropriate controls for all of our studies of the effects of A-bomb radiation exposures, including this one. The estimated radiation doses are based on DS86 with the adjustments that are standard practice at RERF (*15, 16*). Of these individuals, 653 reported for examination between September 2000 and February 2003 (see *Flow Cytometry and Schedule of Measurements* below). We decided to exclude results from 120 of these 653 people who had been diagnosed with cancer from our study. The age, gender and radiation dose of the remaining 533 survivors whose lymphocyte samples were subjected to detailed analysis in our study are listed in Table 1. Blood samples were obtained with the informed consent of the survivors, and PBL were separated by the Ficoll-Hypaque gradient technique (*7*).

In Japan, projects of this type must obtain approval from the appropriate Institutional Ethics Committee prior to the commencement of work. In the case of RERF, the relevant committee at the time this project was carried out was known as the Human Investigation Committee, and its approval was sought and granted before the work was started.

Monoclonal Antibodies (mAbs)

FITC-labeled anti-CD4, biotin-labeled anti-CD4, PerCP-labeled anti-CD4, biotin-labeled anti-CD8, PerCP-labeled anti-CD8, phycoerythrin (PE)-labeled anti-CD8, PE-labeled anti-CD3, PerCP-labeled anti-CD3, FITC-labeled anti-CD57, FITC-labeled anti-TCRαβ, and PE-labeled anti-CD62L mAbs were purchased from BD PharMingen (San Diego, CA). PE-labeled anti-CD45RA mAb and FITC-labeled anti-CD45RO mAb were obtained from Coulter Immunotech (Marseille, France) and Caltag Laboratories (Burlingame, CA), respectively.

Flow Cytometry and Schedule of Measurements

Analytical flow cytometry was conducted in a FACScan machine (BD Biosciences, San Jose, CA). Between September 2000 and February 2003, expression of CD45RO and CD62L was analyzed using a combination of FITC-labeled anti-CD45RO, PE-labeled anti-CD62L, and PerCP-labeled anti-CD4 or PerCP-labeled anti-CD8 mAbs. $CD45RO^-/CD62L^+$, $CD45RO^+/CD62L^+$, $CD45RO^+/CD62L^-$ and $CD45RO^-/CD62L^-$ cell fractions in CD4 and CD8 T-cell populations were determined as shown in Fig. 1. Note that we used only bright CD8 expression to identify CD8 T cells to exclude NK cells, which are dully CD8 positive. The percentages of CD45RA-positive naïve and CD45RA-negative memory CD4 T cells in the PBL fractions were measured between October 1992 and March 1995 (*3*). Analyses of the expression of CD45RA in the CD8 T-cell subset involved staining mononuclear cell fractions with FITC-labeled anti-TCRαβ mAb and PE-labeled anti-CD45RA mAb, and with biotin-labeled anti-CD8 mAb sandwiched by streptavidin-RED670 (Gibco BRL, Rockville, MD); the CD45RA expression was determined for the CD8 and TCRαβ double-positive fraction of the survivors' PBL between October 1992 and March 1995. From April 1997 to April 1999, the expression of CD57 in the CD8 T-cell subsets was analyzed using a combination of PE-labeled anti-CD3, PerCP-labeled anti-CD8, and FITC-labeled anti-CD57mAbs; the CD57 expression was determined for the CD3 and CD8 double-positive fraction. The expression of CD28 in the CD8 T-cell subset was analyzed using a combination of PerCP-labeled anti-CD3, PE-labeled anti-CD8, and FITC-labeled anti-CD28mAbs, and the CD28 expression was determined for the CD3 and CD8 double-positive fraction from May 1999 to April 2001. In every measurement, approximately 20,000 cells were analyzed.

Data Analysis

We used a set of data obtained from individuals whose PBL samples were subjected to examinations of CD45RO and CD62L expression to describe the T-cell subpopulations of all 533 A-bomb survivors. Associations of the percentage of each T-cell subpopulation (*percentage*) with age at the time of examination (*age*), gender and radiation dose (*dose*) were analyzed based on the following multiple regression model (*17*), assuming that the percentage of each T-cell subpopulation was related to each explanatory variable in an exponential manner:

$$\log(percentage) = \alpha + \beta_1 age + \beta_2 gender + \beta_3 dose,$$

where

$$gender = \begin{cases} 0 & \text{for male and} \\ 1 & \text{for female} \end{cases}$$

TABLE 2
Regression Coefficients for Variables Related to the Percentages of CD4 and CD8 T-Cell Subpopulations Expressing Different CD45 Isoforms in PBL among A-Bomb Survivors[a]

Duration of measurements	T-cell subpopulation	Effects			
		Intercept α	Age (10 years)[b] β_1	Gender[c] β_2	Dose (Gy)[d] β_3
September 2000 to February 2003	CD4				
	$CD45RO^-$	4.61	−0.260	0.034	−0.083
			$P = 0.0001$**	$P = 0.56$	$P = 0.036$*
	$CD45RO^+$	3.43	−0.025	0.084	−0.002
			$P = 0.057$	$P = 0.0006$**	$P = 0.92$
	CD8				
	$CD45RO^-$	2.45	−0.098	0.102	−0.063
			$P = 0.0008$**	$P = 0.064$	$P = 0.098$
	$CD45RO^+$	1.98	0.027	−0.077	0.074
			$P = 0.27$	$P = 0.091$	$P = 0.013$*
October 1992 to March 1995	CD4[e]				
	$CD45RA^+$	3.84	−0.124	0.035	−0.054
			$P = 0.0001$**	$P = 0.34$	$P = 0.034$*
	$CD45RA^-$	2.94	0.007	0.65	−0.016
			$P = 0.63$	$P = 0.014$*	$P = 0.35$
	CD8[f]				
	$CD45RA^+$	2.77	−0.065	0.006	0.004
			$P = 0.0053$**	$P = 0.88$	$P = 0.88$
	$CD45RA^-$	1.04	0.022	−0.182	0.043
			$P = 0.49$	$P = 0.0018$**	$P = 0.28$

[a] Regression coefficients of percentage T cells for age, gender and dose were obtained using the following formula: $Percentage\ T\ cells = \alpha + \beta_1 \times age + \beta_2 \times gender + \beta_3 \times dose$.
[b] Effects of age were estimated for 10-year intervals.
[c] Gender = 0 for male and = 1 for female.
[d] Effects of dose were estimated for 1 Gy.
[e] Results for a total of 723 A-bomb survivors have been reported in ref. (*3*), and those for 497 survivors whose data are available for both the current (2000–2003) and previous (1992–1995) studies are presented here.
[f] Results for 497 survivors whose data are available for both the current and previous studies are presented here.
* $P < 0.05$, ** $P < 0.01$.

RESULTS

Three-Color Flow Cytometry Involving CD62L Expression Revealed Effects of A-Bomb Radiation on Naïve CD8 T-Cell Population

Although a dose-dependent decrease in the percentage of naïve CD4 T cells that were enumerated with the $CD45RA^+$ phenotype has been observed repeatedly among A-bomb survivor populations (*3, 7*), radiation effects on naïve CD8 T-cell populations remained to be investigated. Table 2 summarizes the results of CD45RO expression analyses for a total of 533 A-bomb survivors who were examined between September 2000 and February 2003, along with the results of CD45RA expression analyses that were obtained from previous examinations (October 1992 to March 1995). We found high correlations between the current and previous examinations. The correlation coefficients (r) between the percentages of $CD45RO^-$ (current) and $CD45RA^+$ (previous) subsets in CD4 and CD8 T-cell populations were 0.85 ($P = 0.0001$) and 0.68 ($P = 0.0001$), respectively. Between the percentages of $CD45RO^+$ (current) and $CD45RA^-$ (previous) subsets in CD4 and CD8 T-cell populations, r was 0.75 ($P = 0.0001$) and 0.64 ($P = 0.0001$), respectively. This suggested that it would be reasonable to compare the effects of age, gender and radiation dose on these T-cell subsets in the previous and current examinations. As for CD4 T-cell populations, the effects of age, gender and radiation dose on $CD45RO^-$ and $CD45RO^+$ subsets appeared to be virtually in accord with those effects on $CD45RA^+$ and $CD45RA^-$ subsets. There appeared to be a significant effect of radiation on $CD45RO^+$ CD8 T cells in the current examination but not on the counterpart $CD45RA^-$ CD8 T cells in the previous study. At any rate, significant dose-dependent reductions in the percentages of $CD45RO^-$ and $CD45RA^+$ subsets containing naïve cells were apparent for the CD4 but not CD8 T-cell populations of the survivors, probably due to a substantial fraction of memory CD8 T cells included in the $CD45RO^-$ and $CD45RA^+$ subsets (*10, 18, 19*).

In the present study, we intended to discriminate naïve and memory cells in the $CD45RO^-$ subset by using CD62L as the third marker. Figure 1 shows representative flow cytometry patterns that were obtained from two typical male and female survivors who were relatively young and old. It is clear that the $CD45RO^-$ fraction of CD4 T-cell populations consists mostly of $CD62L^+$ cells, whereas there are

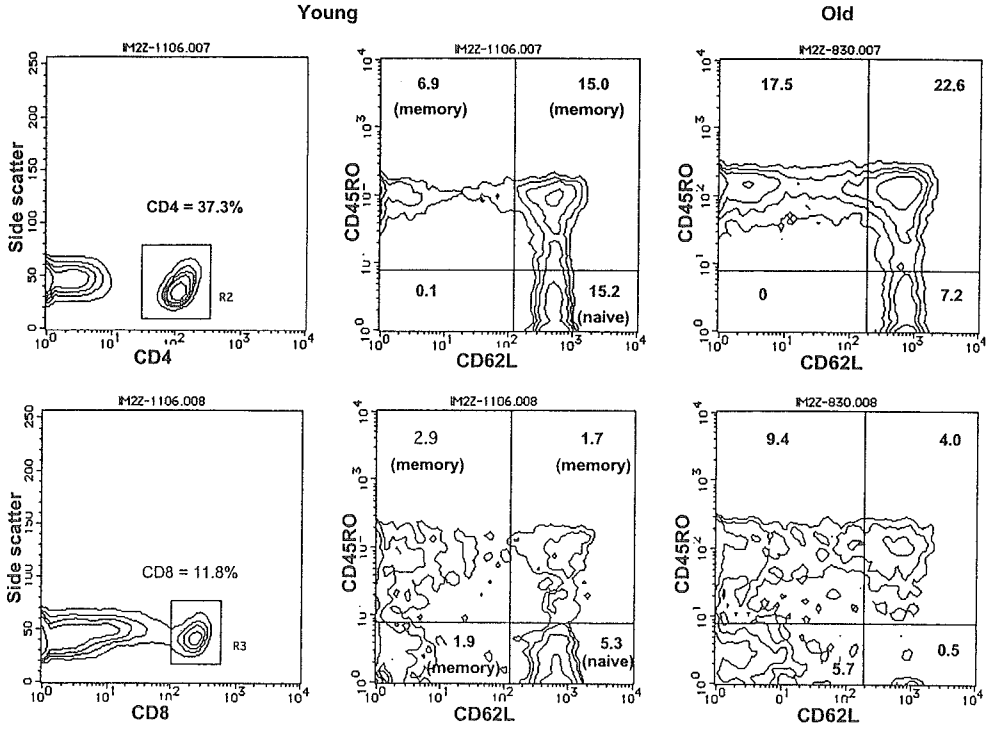

FIG. 1. Flow cytometry patterns of peripheral blood CD4 (upper panel) and CD8 (lower panel) T cells of typical A-bomb survivors who were relatively young (unexposed 58-year-old male, left and center columns) and old (unexposed 93-year-old female, right column), respectively. Peripheral blood mononuclear cells (about 2×10^5) were stained with FITC-labeled anti-CD62L mAb, PE-labeled anti-CD45RO mAb, and PerCP-labeled anti-CD4 mAb (upper panel) or PerCP-labeled anti-CD8 mAb (lower panel). The number in each quadrant indicates the percentage of cells in PBL.

substantial numbers of CD62L$^-$ cells in the CD45RO$^-$ fraction of CD8 T-cell populations. Although there were some individuals who had significant fractions of CD45RO$^-$/CD62L$^-$ cells in their CD4 T-cell populations, we did not obtain any evidence that A-bomb radiation had affected this minor T-cell subset in any obvious way (data not shown). The CD45RO$^+$ fractions of both CD4 and CD8 T-cell populations can also be divided into CD62L$^+$ and CD62L$^-$ subpopulations. Figure 2 depicts the age and dose trends for the percentage of CD45RO$^-$/CD62L$^+$ (naïve) cells in CD4 and CD8 T-cell populations. In the CD4 T-cell populations, the percentage of CD45RO$^-$/CD62L$^+$ (naïve) cells decreased significantly with increased age (25% per 10-year increment, $P = 0.0001$) or radiation dose (9% per gray, $P = 0.034$), almost concordant with that of CD45RA$^+$ or CD45RO$^-$ cells (also see Table 2). As had been expected, the decrease in the percentage of CD45RO$^-$/CD62L$^+$ (naïve) CD8 T cells was also statistically significant, i.e. a 35% decrease with a 10-year increment of age ($P = 0.0001$) and an 8% decrease per gray ($P = 0.031$). These results clearly indicate that the history of radiation exposure has generated a long-lasting reduction of naïve cell pools in both the CD4 and CD8 T-cell populations among A-bomb survivors.

Dose-Dependent Increases in the Percentages of Memory CD8 T-Cell Subsets

The percentage of CD45RO$^+$ CD8 memory T cells appeared to increase significantly with radiation dose (Table 2). This was not obvious in the measurement with CD45RA, which was used as a naïve/memory marker. To describe the memory T-cell subsets in this study, we determined two distinct CD62L$^+$ and CD62L$^-$ compartments in CD45RO$^+$ cells in both CD4 and CD8 T-cell populations, along with an additional CD62L$^-$ compartment in the CD45RO$^-$ CD8 T-cell population (Fig. 1). It has been reported that memory T cells in the CD62L$^+$ compartment have an increased potential to proliferate in response to recall antigens *in vitro* and a greater capacity to persist *in vivo* than memory T cells in the CD62L$^-$ compartment (*20, 21*). For CD4 but not CD8 T-cell populations, the percentages of CD45RO$^+$/CD62L$^+$ memory T cells in PBL were found to decrease significantly with increasing age of the A-bomb survivors (Fig. 3 and Table 3). We also found dose-dependent increases in the percentages of CD45RO$^+$/CD62L$^+$ CD8 T cells (12% increase per gray, $P = 0.0055$) and CD45RO$^+$/CD62L$^-$ CD8 T cells (8% increase per gray, $P = 0.034$), which were not found for the CD45RO$^+$/

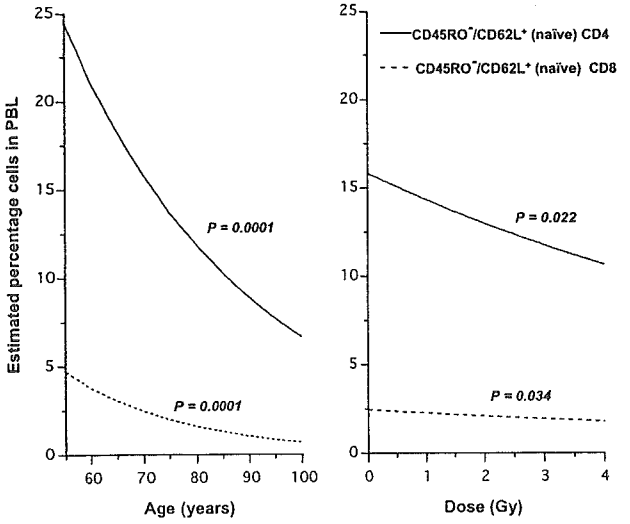

FIG. 2. Estimated radiation dose responses in the percentages of naïve ($CD45RO^-/CD62L^+$) CD4 and CD8 T cells in PBL among 533 A-bomb survivors. The values were adjusted to those of unexposed males or 70-year-old males and plotted as a function of age (left panel) or radiation dose (right panel), respectively, according to the formula described in the Materials and Methods.

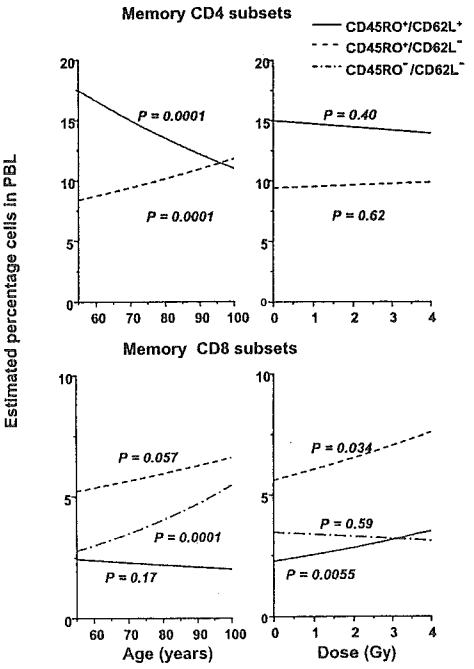

FIG. 3. Estimated radiation dose responses in the percentages of memory CD4 (upper panel) and CD8 (lower panel) T-cell subsets in PBL among 533 A-bomb survivors. The values were adjusted to those of unexposed males or 70-year-old males and plotted as a function of age (left panels) or radiation dose (right panels), respectively, according to the formula described in the Materials and Methods.

$CD62L^+$ or $CD45RO^+/CD62L^-$ CD4 T cells among the same survivors. There was no effect of dose on $CD45RO^-/CD62L^-$ cells in CD8 T-cell populations. These results indicate that the history of radiation exposure has dose-dependently caused increases in subsets ($CD45RO^+/CD62L^+$ and $CD45RO^+/CD62L^-$) of memory CD8 T cells among A-bomb survivors.

Increased Percentages of $CD45RO^+/CD62L^+$ or $CD45RO^+/CD62L^-$ CD8 T Cells by Radiation Exposure may not be Restricted to$CD28^-$ or $CD57^+$ T Cells

Other studies have reported that clonal expansion of a subset of CD8 T cells, such as $CD28^-$ or $CD57^+$, occurred frequently in older individuals (*22–25*). To test whether the increased percentage of $CD45RO^+/CD62L^+$ or $CD45RO^+/CD62L^-$ CD8 T cells that we observed among the survivors was associated with expansion of CD28-negative or CD57-positive cell populations, we analyzed the effects of age, gender and dose on the percentages of $CD28^-$ and $CD57^+$ CD8 T cells and examined the correlations among $CD28^-$, $CD57^+$, $CD45RO^+/CD62L^+$, and $CD45RO^+/CD62L^-$ CD8 T cells (Table 4). The percentages of $CD28^-$ and $CD57^+$ CD8 T cells were much less correlated with those of $CD45RO^+/CD62L^+$ CD8 T cells (r = 0.18 and 0.22, respectively) than those of $CD45RO^+/CD62L^-$ CD8 T cells (r = 0.62 and 0.60, respectively). This could indicate that expansion of $CD45RO^+/CD62L^-$ CD8 T cells is associated with increased proportions of $CD28^-$ or $CD57^+$ CD8 T cells. However, no significant effect of A-bomb radiation on $CD28^-$ or $CD57^+$ CD8 T cells was found, although there did appear to be a remarkable increase with age in the percentage of these subsets. Thus it is implied that the increased percentages of $CD45RO^+/CD62L^+$ and $CD45RO^+/CD62L^-$ CD8 T cells with increased radiation dose may not be largely due to increases in the percentages of $CD28^-$ and $CD57^+$ CD8 T cells.

DISCUSSION

Our present findings clearly indicate that radiation exposure has reduced the size of naïve cell pools not only in CD4 T-cell populations but also in the other major T-cell subset, CD8, among A-bomb survivors. One of the most plausible explanations for this is that the reduction in the size of naïve T-cell pools could have resulted from an insufficient supply of new T cells from the thymus since the majority of the naïve T cells develop in the thymus. Recently, it has been reported that the numbers of recent thymic emigrant cells can be determined in T-cell populations by detecting T lymphocytes that contain T-cell receptor-rearrangement excision circles (TRECs), which are circular DNA molecules generated in thymocytes during the T-cell receptor gene rearrangement process in the thymus (*26*). It has also been reported that significantly fewer CD4 T cells containing TRECs are currently demonstrable in bone marrow transplantation patients who were exposed to whole-body irradiation more than 20 years ago (*27*). Thus it is

TABLE 3
Regression Coefficients for Variables Related to the Percentages of CD4 and CD8 T-Cell Subpopulations Expressing Different Levels of CD62L in PBL among A-Bomb Survivors[a]

T-cell subpopulation	Effects			
	Intercept α	Age (10 years)[b] β_1	Gender[c] β_2	Dose (Gy)[d] β_3
CD4				
$CD45RO^-/CD62L^+$	4.79	−0.290	0.022	−0.099
		$P = 0.0001$**	$P = 0.72$	$P = 0.022$*
$CD45RO^+/CD62L^+$	3.43	−0.104	0.096	−0.019
		$P = 0.0001$**	$P = 0.0037$**	$P = 0.40$
$CD45RO^+/CD62L^-$	1.71	0.076	0.070	0.012
		$P = 0.0001$**	$P = 0.046$*	$P = 0.62$
CD8				
$CD45RO^-/CD62L^+$	3.92	−0.432	0.170	−0.081
		$P = 0.0001$**	$P = 0.0020$**	$P = 0.034$*
$CD45RO^+/CD62L^+$	1.11	−0.042	0.025	0.109
		$P = 0.17$	$P = 0.66$	$P = 0.0055$**
$CD45RO^+/CD62L^-$	1.37	0.052	−0.116	0.075
		$P = 0.057$	$P = 0.025$*	$P = 0.034$*
$CD45RO^-/CD62L^-$	0.188	0.151	−0.007	−0.027
		$P = 0.0001$**	$P = 0.93$	$P = 0.59$

[a] Regression coefficients of percentage T cells for age, gender and dose were obtained using the following formula: *Percentage T cells* $= \alpha + \beta_1 \times age + \beta_2 \times gender + \beta_3 \times dose$.
[b] Effects of age were estimated for 10-year intervals.
[c] Gender = 0 for male and 1 for female.
[d] Effects of dose were estimated for 1 Gy.
* $P < 0.05$, ** $P < 0.01$.

expected that a similar reduction in the number of recent thymic emigrant cells would be observed among A-bomb survivor populations. Therefore, we recently started measuring the numbers of recent thymic emigrant cells that can be detected in both the CD4 and CD8 T-cell populations of A-bomb survivors with a view to determining whether a reduced production of new T cells in the thymus is an actual cause of the impaired maintenance of naïve T-cell pools among survivors. Another plausible mechanism is that the reduction of the naïve cell pool size might have resulted from the homeostatic and/or antigenic proliferation of naïve T-cell populations followed by their transfer to memory T-cell pools. We are also planning to analyze the turnover of naïve CD4 T-cell populations by tracking genetically marked murine naïve CD4 T cells after implantation into irradiated mice. Such an experimental model will provide us with valuable information for a precise understanding of what happens when radiation exposure seriously impairs the ability of irradiated hosts to maintain normal-sized naïve CD4 T-cell pools.

In most individuals, CD62L-negative cells are undetectable among $CD45RO^-$ CD4 T-cell populations while $CD45RO^-$ CD8 T-cell populations contain a significant fraction of CD62L-negative cells that are known to exhibit potential effector functions (*10–14*). We found that the percentages of $CD45RO^-/CD62L^-$ CD8 T cells increased with age (Fig. 3, Table 3). Although the meaning of this age dependence is unclear, it is not inconceivable that frequent antigen exposures due to decreased immunocompetence in aged individuals leads to an accumulation of effector T-cell populations.

Recent studies suggest that $CD45RA^-(CD45RO^+)$ memory T cells are heterogeneous in their functions and that they comprise distinct populations (*21, 22, 28–34*). These memory subsets can also be distinguished based on the expression of other surface markers, including CD62L (*21, 30, 32, 33*). In addition to impairment in the maintenance of naïve cell pools, our results also suggest that A-bomb radiation has induced a change in the memory T-cell pools of the survivors' CD8 T-cell populations that involves a dose-dependent increase in the percentage of $CD45RO^+/CD62L^+$ or $CD45RO^+/CD62L^-$ cells. Sallusto *et al.* (*28*) have recently proposed that memory ($CD45RA^-$ and $CD45RO^+$) T cells can be classified into central ($CCR7^+$ and mostly $CD62L^+$) and effector ($CCR7^-$ and mostly $CD62L^-$) memory T cells. These subsets were found to show several differences in their functions (*34*), migration capacities (*28*), proliferation abilities (*21, 22, 32*), telomere lengths (*21*), and T-cell receptor repertoires (*33*). These findings suggest that effector memory T cells are immature compared to central memory T cells (*35*), although it is unclear whether the latter memory subset stems from the former (*33, 36*).

Here we discuss possible reasons that the radiation effect is apparent for both the central and effector CD8 memory T-cell subsets. One possible interpretation is that the entry